Published in final edited form as:
Nat Metab. 2019 May ; 1(5): 532–545. doi:10.1038/s42255-019-0059-2.

Branched chain amino acids impact health and lifespan indirectly via amino acid balance and appetite control

Samantha M Solon-Biet[1,2,*], **Victoria C Cogger**[1,3,4,9], **Tamara Pulpitel**[1,3], **Devin Wahl**[1,3,4], **Ximonie Clark**[1,2], **Elena Bagley**[1,5], **Gabrielle C Gregoriou**[1,5], **Alistair M Senior**[1,2], **Qiao-Ping Wang**[1,2,12], **Amanda E Brandon**[1,3], **Ruth Perks**[1], **John O'Sullivan**[1,6], **Yen Chin Koay**[1,6], **Kim Bell-Anderson**[1,2], **Melkam Kebede**[1,2], **Belinda Yau**[1,2], **Clare Atkinson**[1,2], **Gunbjorg Svineng**[7], **Timothy Dodgson**[1,2], **Jibran A Wali**[1,2], **Matthew D W Piper**[8], **Paula Juricic**[10], **Linda Partridge**[10], **Adam J Rose**[11], **David Raubenheimer**[1,2], **Gregory J Cooney**[1,3], **David G Le Couteur**[1,3,4,9], **Stephen J Simpson**[1,2,*]

[1]Charles Perkins Centre, The University of Sydney NSW, Australia

[2]School of Life and Environmental Sciences, Faculty of Science, The University of Sydney, NSW, Australia

[3]Sydney Medical School, Faculty of Health and Medicine, The University of Sydney NSW, Australia

[4]Ageing and Alzheimers Institute and Centre for Education and Research on Ageing, Concord Hospital, Concord NSW, Australia

[5]School of Medical Sciences, Faculty of Health and Medicine, The University of Sydney NSW, Australia

[6]Heart Research Institute, The University of Sydney, NSW, Australia

[7]Department of Medical Biology, The Arctic University of Tromso

[8]School of Biological Sciences, Monash University VIC, Australia

[9]ANZAC Research Institute, The University of Sydney NSW, Australia

[10]Max Planck Institute for Biology of Aging, Cologne, Germany

[11]Monash Biomedicine Discovery Institute, Monash University VIC, Australia

[12]School of Pharmaceutical Sciences (Shenzhen), Sun Yat-Sen University, Guangzhou 510275, China

[*]Correspondence can be addressed to: stephen.simpson@sydney.edu.au or samantha.biet@sydney.edu.au.

Author contributions

DLC, SJS, LP conceived the study. SSB, SJS, DLC wrote the manuscript. DR, LP and AJR reviewed and assisted in writing the manuscript. SSB, VCC and TP ran the study. GJC, DW, XC, AEB, EB, GCC, RP, JOS, YK, MK, BY, CA, GS, TD, JAW, PJ ran experiments. SSB, AMS, QW, KBA, MDWP, PJ analyzed data.

Declaration of Interests

The authors declare no competing interests.

Data availability

RNAseq data have been deposited in NCBI's Gene Expression Omnibus and are accessible through GEO Series accession number GSE114855. The data that support the plots within this paper and other findings of this study are available from the corresponding author upon reasonable request.

Summary

Elevated branched chain amino acids (BCAAs) are associated with obesity and insulin resistance. How long-term dietary BCAAs impact late-life health and lifespan is unknown. Here, we show that when dietary BCAAs are varied against a fixed, isocaloric macronutrient background, long-term exposure to high BCAA diets leads to hyperphagia, obesity and reduced lifespan. These effects are not due to elevated BCAA *per se* or hepatic mTOR activation, but rather due to a shift in the relative quantity of dietary BCAAs and other AAs, notably tryptophan and threonine. Increasing the ratio of BCAAs to these AAs resulted in hyperphagia and is associated with central serotonin depletion. Preventing hyperphagia by calorie restriction or pair-feeding averts the health costs of a high BCAA diet. Our data highlight a role for amino acid quality in energy balance and show that health costs of chronic high BCAA intakes need not be due to intrinsic toxicity but, rather, a consequence of hyperphagia driven by AA imbalance.

Keywords

Nutrition; metabolic health; aging; branched chain amino acids; obesity; dietary balance; dietary restriction; lifespan; appetite; serotonin

Introduction

The role of macronutrients (proteins, fats and carbohydrates) in linking diets to health has been the focus of much research. Recent work has underscored the necessity of examining these links within a mixture framework, which is sensitive not only to the individual effects of macronutrients, but also their interactive effects [1]. Protein, in particular, has been shown to interact powerfully with dietary fats and carbohydrates to influence health via effects on appetite and post-ingestive physiology. One such interaction, observed in many animals including humans, is ‘protein leverage’, in which the strong appetite for protein causes the over-consumption of fats and carbohydrates when feeding on protein-dilute diets [2,3]. Another is the demonstration that the dietary ratio of protein to carbohydrate impacts reproduction, aging, immune function, microbiome, late-life cardiometabolic health, brain health and lifespan [4–7].

Proteins, however, are themselves complex mixtures of amino acids (AA) that when modified, can have profound effects on growth, early life health and longevity [8–10]. Restriction of specific AAs, such as methionine, mimic the health and lifespan effects of chronic dietary restriction, despite an increase in energy intake [11]. Indeed, most AAs have important functions in metabolic health outside their role in protein synthesis. The branched chain amino acids (BCAAs: isoleucine, leucine and valine) have assumed particular prominence, both because of their role in influencing insulin, insulin-like growth factor (IGF-1) and mechanistic target of rapamycin (mTOR); key pathways linking nutrition with health and aging [12], and also because their circulating levels are positively associated with obesity, insulin resistance and metabolic dysfunction in rodents [5,13–16] and are associated with obesity, insulin resistance and type 2 diabetes in humans [17–20]. We previously reported that mice fed a high protein, low carbohydrate diet throughout life were hypophagic, metabolically impaired in latelife, had elevated circulating BCAAs, increased hepatic mTOR

activation and reduced median lifespans compared to mice fed a low protein, high carbohydrate diet [5]. These results suggest that health and aging in mice can be altered by titrating the balance of macronutrients to influence circulating BCAAs and mTOR activation.

Here, we sought to determine whether and how dietary BCAA manipulation influences healthspan and lifespan in mice. We demonstrate that the metabolic and lifespan costs of high BCAA: non-BCAA intakes, when paired with a high carbohydrate, low fat nutritional background, are not associated with increased hepatic mTOR activation, but rather, can be explained by their interactions with other key metabolically essential AAs leading to extreme hyperphagia. Rebalancing the AA profile in the diet with the addition of tryptophan (Trp) or threonine (Thr) suppressed food intake while preventing hyperphagia on BCAA-supplemented diets by either 20% calorie restriction (CR) or pair-feeding reversed metabolic dysfunction and lifespan costs. These findings illustrate the complex nutritional interactions that influence appetite signaling, metabolic health and lifespan in mice.

Results

Dietary AA imbalance drives hyperphagia and shortens lifespan

312 male and female C57BL/6J mice were fed one of four isocaloric diets (all 18% total protein, 64% carbohydrate, 18% fat, total energy density 14.3 kJ/g) varying in protein quality and amino acid (AA) balance. Mice were either euthanized at 15 months of age for tissue analysis or maintained for lifespan determination. Data shown are the averages of males and females combined, unless otherwise stated for variables that showed a statistically significant sex difference. Manipulations to protein quality were performed so that the BCAA200 diet contained twice the BCAAs of the control diet BCAA100 (AIN93-G), which contains the standard amount of BCAAs. The BCAA50 and BCAA20 diets contained one half and one fifth of standard content of BCAAs, respectively. These adjustments to BCAAs resulted in a change in the ratio of BCAAs to other AAs (henceforth, ‘non-BCAAs’) within the fixed total protein complement of 18% (Supplementary Table 1). Mice confined to the BCAA200 diets (i.e. the diet with highest ratio of BCAA to non-BCAA) were hyperphagic, consuming ~20% more energy than mice on other diets (Fig. 1a). When non-BCAA intake was plotted, mice on all treatment groups, except BCAA200, maintained their average intake of non-BCAAs to a similar level, suggesting regulation of intake of one or more non-BCAAs to a target intake, with BCAA and total energy intakes following passively (Fig. 1b).

We hypothesized that one or more non-BCAAs were regulated to a target intake and if this target could not be met due to dietary imbalance, mice overconsumed food (and consequently both total energy and BCAAs) to reach this intake target. As a result of such compensatory feeding, hyperphagic mice had significantly increased body weight and fat mass with no change in lean mass (Fig.1c-g). Circulating levels of the BCAAs were strongly associated with BCAA intake, plateauing at approximately 40 μg/ml (Fig. 1h). Plasma BCAAs of mice on BCAA200 and BCAA100 diets did not differ (Supplementary Fig. 4h), despite hyperphagia and the doubling of BCAA content in the BCAA200 diet, suggesting that the blood levels of BCAAs are regulated post-ingestively. Adiposity was strongly associated with circulating BCAA levels (Fig. 1i) and supported by elevated leptin levels in

mice fed a BCAA200 diet (Fig. 1j). Elevated circulating leptin was not accompanied by changes in hypothalamic gene expression of *Lepr* or *Socs3,* key features of leptin resistance seen in many obese animals (Supplementary Fig. 2c,d).

Given that BCAAs activate the mTOR signaling pathway, we quantified activation of mTOR, S6K and AKT in the liver and found few differences between groups (Fig. 1k-m), which may be attributed to the dietary macronutrient background on which BCAAs were manipulated (i.e. high carbohydrate, low fat). Despite no increase in hepatic mTOR activation, median lifespan of BCAA200 mice was reduced by ~10% when compared to the other dietary groups (Fig. 1n; BCAA200: 92.8w, BCAA100: 102.3w, BCAA50: 102.6w, BCAA20: 104.6w; all comparisons $p<0.05$), which are likely due to the effects of hyperphagia and obesity.

Rebalancing the BCAA200 diet with Trp and Thr prevents hyperphagia

To determine whether there were specific non-BCAAs that mediated this effect, the intake of each essential AA (EAA) was calculated [21,22]. The ratio among AAs in the non-BCAA complement were not identical between treatment diets (Supplementary Table 1), offering the opportunity to disentangle non-BCAA effects. The intakes of three EAAs, Trp, Thr and methionine (Met), were maintained consistently across diet treatments (Fig. 2a), suggesting that these AAs are prioritized and regulated, influencing food intake and feeding behavior.

We next tested the hypothesis that there is an intake target for one or more of these three EAAs, which mice will attempt to achieve despite the overconsumption of energy and BCAAs, as observed in BCAA200 mice. A six-week intervention was performed where mice were fed BCAA200 diets supplemented with either Met, Thr or Trp (by 150% of standard chow concentrations thereby normalizing the ratio between these individual AAs and dietary BCAAs; Supplementary Table 2). Supplementation of Trp or Thr, two metabolically essential AAs [22], but not Met, suppressed food intake on BCAA200 diets towards levels seen in control mice on the BCAA100 diet (Fig. 2b). When matched to the exome [23], Trp and Thr, but not Met, were the limiting AA on BCAA200 diets (Supplementary Fig. 1). These results imply that food intake can be regulated by the interaction between BCAAs, Trp and Thr, whereby addition of these EAAs largely reversed the hyperphagia induced by imbalanced high BCAA diets by normalizing their ratio.

Hyperphagia is linked to Trp-mediated serotonin (5HT) depletion

Plasma metabolomics was performed using targeted LC-QQQ-MS and showed that glutathione metabolism and aminoacyl-tRNA synthesis pathways were positively associated with high BCAA: non-BCAA intakes, while TCA cycle and Trp metabolism pathways were negatively associated (Fig. 3a,b and Supplementary Table 3). The downregulation of Trp metabolism is of particular importance in feeding behavior as Trp is the sole precursor for the production of 5-hydroxytryptamine (5HT, serotonin), a monoamine neurotransmitter that controls appetite. The reduction in Trp, 5HT and its main metabolite 5-hydroxyindoleacetic acid (5-HIAA) in plasma of mice with high BCAA: non-BCAA intakes reflect peripheral Trp limitation (Fig. 3c). Indeed, the inverse relationship between BCAAs and Trp, which compete for peripheral and central transport [24] by the L-type AA transporter LAT1

(SLC7A5) [25] is also reflected in the ratio of Trp:BCAA in plasma and cortex, where BCAA200 mice exhibit the lowest Trp:BCAA ratio (Fig. 3d).

To determine if reduced Trp:BCAA ratio in plasma and cortex reflect central Trp-mediated 5HT depletion, we fed mice for six weeks on either the BCAA200 diet or the BCAA100 diet as a control. We made patch clamp recordings from dorsal raphe neurons and electrically stimulated locally to evoke the synaptic release of 5HT (Fig. 3e). Stimulation in the dorsal raphe evoked an inhibitory post-synaptic current (eIPSC) in control BCAA100 mice (shown in black), that was blocked by the 5HT1A receptor antagonist NAN-190 (shown in blue). BCAA200 mice showed significantly blunted eIPSC upon stimulation, consistent with the hypothesized diet-related 5HT depletion. Average eIPSC amplitude was significantly lower in BCAA200 mice compared to BCAA100 mice ($p<0.001$), the response of which was rescued by the addition of Trp in media (Fig. 3f). This suggests that increased dietary BCAAs, relative to Trp, is sufficient to lower Trp availability for central Trp uptake and 5HT synthesis. We then tested if increasing 5HT availability in the brain would reduce food intake in mice on a BCAA200 diet. An additional group of mice was fed for six weeks on the BCAA200 diet and treated with either saline or fluoxetine, a widely used antidepressant and selective serotonin reuptake inhibitor (SSRI), via oral gavage for four days. Mice treated with fluoxetine showed a rapid and significant decrease in food intake compared to saline controls from day one of treatment (Fig. 3g), a pattern that persisted for the next three days.

High BCAA: non-BCAA intake alters hypothalamic gene expression

To investigate how dietary BCAA: non-BCAA influences central appetite signaling, we performed RNAseq in the hypothalamus of 15 month old mice. Differentially expressed genes were correlated with BCAA intake and genes with significant correlations were plotted on a heatmap. Mice with the highest intake of BCAAs (and hence low non-BCAA intake) had a contrasting pattern of gene expression compared with all other mice (Fig. 4a). Three genes, *Dyrk1a, Ttc7b and Nlrp3* (previously linked with appetite, obesity and inflammation, respectively) showed strong positive correlations with high BCAA intakes (Fig. 4b). Transgenic mice with increased hypothalamic *Dyrk1a* mRNA expression exhibit increased food intake [26] which is mediated by FOXO-induced *Npy* expression, a key gene in the orexigenic pathway that regulates appetite. *Ttc7b* expression, a marker of fat cell function and lipid storage, was elevated with high BCAA: non-BCAA intakes, together with an increase in the inflammasome marker *Nlrp3* (Fig. 4b) [27,28]. Functional annotation revealed that genes positively associated with high BCAA: non-BCAA intakes were enriched in several pathways related to cancer while negatively associated pathways included p53 signaling and apoptotic pathways (Fig. 4c). These pathways showed significant EASE Scores [29]; however, after adjusting for multiple testing, these pathways did not remain significant (Supplementary Table 4).

High BCAA: non-BCAA diets promote hepatosteatosis and de novo lipogenesis

Hyperphagic mice on BCAA200 diets developed hepatosteatosis (Fig. 5a). Hepatic triglyceride content, fat scores and levels of plasma α-keto-δ-(NGNG-dimethylguanidino)-valeric acid (DMGV, a human metabolite recently found to be a biomarker for non-alcoholic fatty liver disease [30]), were significantly elevated in BCAA200 mice (Fig. 5b-d and

Supplementary Table 5) and supported by elevations in plasma ALT and AST (Fig. 5e,f; Supplementary Fig. 3b,c and Supplementary Table 5). Markers of hepatic *de novo* lipogenesis were decreased in BCAA20 diets. These include ATP citrate lyase (ACLY), stearoyl-CoA desaturase-1 (SCD1), fatty acid synthase (FAS) and acetyl-CoA carboxylase (ACC) (Fig. 5g,h). Excess BCAAs may contribute directly to *de novo* lipogenesis [31] or via increased ACLY phosphorylation by the branched-chain ketoacid dehydrogenase kinase (BDK) [32].

Dietary BCAA: non-BCAA imbalance alters whole body metabolism

No differences in energy expenditure were detected among groups (EE; Fig. 6a, Supplementary Fig. 3h and Supplementary Table 5), nor were there differences in UCP1 protein expression (Fig. 6c). When UCP1 expression was normalized for BAT mass, BCAA200 mice showed reduced UCP1 expression (Fig. 6d). Preferential oxidation of carbohydrate fuels by BCAA20 mice is indicated by increased respiratory quotient (RQ; Fig. 6b) and supported by elevated hepatic *Pepck* mRNA expression (Fig. 6e), a marker of gluconeogenesis. BCAA20 mice also showed increased pancreatic islet glucagon content (Fig. 6 f,g), a hormone which signals hepatic conversion and release of glucose from glycogen, a process central to the regulation of blood glucose levels. Increased glucagon in BCAA20 mice corresponds to the observed reduced fasting insulin levels and pancreas mass (Fig. 6h, Supplementary Fig. 2f), which persisted despite increased islet area and no change in islet insulin content (Supplementary Fig. 2g-h). We found no differences in basal blood glucose levels or glucose tolerance, but found a significant positive relationship between plasma BCAAs and the product of fasting glucose and insulin, an index of insulin sensitivity (Fig. 6i-l). Additionally, plasma triglycerides and plasma IGF1 levels did not differ across groups (Fig. 6m,n). FGF21 levels were not significantly different across diets when males and females were combined (Supplementary Fig. 2j), but showed a significant sex-by-diet interaction, with diet significantly affecting plasma FGF21 in males (FGF21 being elevated on BCAA200), but not females (Supplementary Fig. 3a and Supplementary Table 5). FGF21 resistance is unlikely as mRNA expression of downstream regulatory co-receptors *Fgfr1c* and *Klb* in white adipose tissue, the proposed site of FGF21 resistance (Supplementary Fig. 2e and Supplementary Fig. 3g), did not differ between groups. Rather, elevated FGF21 levels may reflect AA imbalance and/or limitation on high BCAA: non-BCAA diets, rather than a FGF21-resistant state.

The health impacts of high BCAA: non-BCAA intakes are a consequence of hyperphagia

Our results suggest that the negative health and lifespan costs of long-term high BCAA: non-BCAA diets are a consequence of hyperphagia and obesity, rather than any intrinsic toxicity. Obese mice on a BCAA200 diet have elevated circulating BCAAs and metabolites linked with poor cardiometabolic outcomes [14,33–36]. However, mice on BCAA100 diets with similar levels of circulating BCAAs (Supplementary Fig. 4h) did not exhibit hyperphagia, metabolic dysfunction or shortened lifespan, suggesting that circulating BCAA levels alone cannot predict metabolic health and lifespan. The question therefore arises as to how much of the negative impact of high BCAA intakes on health and lifespan is the result of BCAAs *per se*, and how much is a consequence of hyperphagia?

To distinguish between these alternatives, we explored whether preventing hyperphagia by either 20% calorie restriction (CR) or pair-feeding would prevent metabolic and lifespan costs observed in *ad libitum*-fed mice on BCAA-supplemented diets. A separate cohort of mice was fed across the life-course on BCAA200 and BCAA100 diets provided as a single aliquot of food per day (80% of the *ad libitum* intake of BCAA100 mice). CR increased median lifespans by approximately 30% relative to *ad libitum*-fed controls on both BCAA200 and BCAA100 diets (Fig. 7a; 134.8 vs 92.8 w on BCAA200 and 143.7 vs 102.3 w on BCAA100, respectively). While *ad libitum*-fed BCAA200 animals lived 10% shorter than *ad libitum*-fed BCAA100 mice (p=0.01), under CR, this difference was reduced to 6% (Fig. 7a; CR200 134.8w vs CR100 143.7w; p=0.68). Preventing hyperphagia on a BCAA200 diet by 20% CR resulted in a reduction in body weight and % body fat (Fig. 7b,c) and led to a reduction of liver triglyceride content, fasting insulin, plasma IGF1 and plasma BCAAs (Fig. 7d-g). Body composition and metabolic differences apparent between BCAA200 and BCAA100 animals under *ad libitum* feeding conditions were mostly normalized under CR (Supplementary Fig. 5a-i), including no difference in circulating BCAAs between 200CR and 100CR groups (Supplementary Fig. 5c). Preventing hyperphagia by pair-feeding also showed that despite dietary BCAA-supplementation, mice did not differ in body weight, develop obesity or show a reduction in lifespan (Fig. 7 h-j; median lifespans 94w for P23, 110w for P6 and 115.5w for P6+BCAA). Together, these data show that the metabolic and lifespan consequences of a high BCAA: non-BCAA diet are not due to BCAAs *per* se, but predominantly a result of hyperphagia.

Discussion

Here, we show that long-term high BCAA: non-BCAA intakes led to hyperphagia, obesity, altered appetite signaling and reduced lifespan. Additionally, we show that elevated circulating BCAAs can occur in both metabolically healthy and unhealthy obese and insulin resistant mice; therefore increased circulating BCAAs alone cannot predict metabolic dysfunction. Given that elevated circulating levels of BCAAs in humans have been reported as biomarkers for obesity [14,37], hepatosteatosis [38,39], insulin resistance [17,18,20,35] and type 2 diabetes [19,33,40], the question arises whether this widely reported relationship between elevated levels of circulating BCAAs and adverse health outcomes reflect intrinsic BCAA toxicity, dietary intakes, or metabolic dysfunction. Although some studies report no difference in circulating BCAAs after whey protein supplementation in humans [18], others show that circulating BCAAs are increased in overfeeding and can be uncoupled from health [41]. Across different strains of mice, BCAAs alone were not identified as the top metabolites associated with insulin resistance [42]. Similarly, our data show that elevated intakes and corresponding circulating levels of BCAAs are not toxic or by themselves markers of insulin resistance, but rather, the major deleterious effects of excess BCAAs under an isocaloric-density, moderate-protein, high-carbohydrate, low-fat background, arise indirectly via hyperphagia and obesity.

We discovered that the metabolic burden of dietary BCAAs under high carbohydrate intakes was not due to increased hepatic mTOR activation, but primarily driven by hyperphagia. Creating dietary imbalance by increasing the ratio of BCAA:non-BCAAs (particularly Trp and Thr) resulted in compensatory feeding and increased energy intake in an attempt to meet

specific non-BCAA intake targets. Recognizing dietary AA imbalance and deficiency has been shown to occur via the uncharged t-RNAs that signal deficiency in forebrain areas such as the anterior piriform cortex (APC) which activates phosphorylation of GCN2 to trigger the amino acid response to promote catabolism and inhibit anabolism [12,43]. In rats, diets devoid or deficient in one or more EAAs result in growth failure and rejection of the diet [10,43], a finding likely linked to extreme deficiency of an indispensable amino acid [22]. However, under *ad libitum* feeding conditions with less severe AA imbalance, compensatory feeding mechanisms increase food intake to obtain target intakes of limiting AAs, rather than cause food aversion – a result reported in early work in rats by Rose [44].

Preventing hyperphagia by 20% CR averted obesity and the metabolic and lifespan costs associated with high BCAA: non-BCAA diets. Similarly, preventing hyperphagia on BCAA-supplemented diets by pair-feeding averted body fat gain and did not shorten lifespan relative to non BCAA-supplemented diets with the same total protein content. Together, these results indicate that: first, dietary BCAAs do not appear to be intrinsically harmful but rather, the adverse health effects can be explained by their interactions with other AAs leading to extreme hyperphagia; and second, that high circulating BCAA concentrations can occur in both metabolically healthy and unhealthy mice, suggesting that BCAAs *alone* are not a sufficient marker of metabolic health.

When considered in light of present results, it is difficult to attribute causality to the relationship between BCAAs and health from previous studies, given that some reports linking elevated levels of circulating BCAAs with metabolic dysfunction in humans show concomitant increases in energy, total protein and/or BCAA intakes [13,14,33,34,36]. In rodents, circulating levels of BCAAs have also been shown to be positively associated with total protein intake [5,15]. In humans, fasting BCAA levels in the obese, insulin-resistant state are attributed to changes in BCAA catabolic enzymes and perturbations in amino acid homeostasis [45]. For example, changes in mTOR signaling in muscle and alterations in branched-chain-amino-acid transaminase (BCATm) (the rate-controlling and irreversible step in BCAA metabolism) and branched-chain α-ketoacid dehydrogenase (BCKD), the mitochondrial BCAA oxidation checkpoint [17], have been shown to link circulating BCAAs and insulin resistance or type 2 diabetes. In this study, we did not find any differences in hepatic mTOR activation, BCAA metabolism, measured by hepatic and skeletal muscle mRNA expression of *Bcat2* (gene encoding BCATm), *Bckdha*, *Bckdhb*, or related metabolites such as the branched-chain-α ketoacids, acylcarnitines or amino acids Phe, Tyr or Glu [14] (Supplementary Fig. 4). This lack of response may be attributed to the dietary macronutrient background on which BCAAs are manipulated whereby alterations to AA balance were conducted under a moderate protein, high carbohydrate, low fat macronutrient background. We have previously shown that maximal hepatic mTOR activation occurred under a combination of high protein and low carbohydrate intakes. It follows that high levels of circulating BCAAs may therefore be associated with poor health outcomes because they reflect long term elevated protein intake, the impacts of which are especially pronounced when coupled with low carbohydrate intakes [5]. Others have also shown that mTOR in rats is increased with BCAA supplementation only when combined with a diet high in fat [14], and that the interaction between high BCAAs and excess dietary fat is central to the development of insulin resistance [46]. Overall, therefore, previous studies are consistent with the concept

that circulating BCAAs reflect health, but the relationship may be more complex than originally postulated. We show that circulating BCAAs are biomarkers for diet, particularly protein and total food intake, and that elevations in circulating BCAAs occur in both metabolically healthy and unhealthy animals. Recent work by Elshorbagy, et al. [41] supports this conclusion, showing that a 28-day intervention of calorie overfeeding in healthy men and women with a BMI of 26.6 ± 0.6 resulted in elevated fasting serum isoleucine and valine by day 3 in the absence of obesity, insulin resistance or type 2 diabetes. However, it is important to note that elevated circulating BCAAs have been associated with improved health in some settings [47–50]. In the short term, high levels of BCAAs caused by high protein intake may be associated with improved outcomes in overweight subjects secondary to protein-leverage-induced weight loss. Additionally, the anabolic effects of elevated BCAA and protein intakes are clearly beneficial for supporting growth and reproduction at appropriate life stages.

The impact of dietary BCAAs on food intake was mediated via interactions with other dietary AAs. We identified stable intakes for three other EAAs, Trp, Thr and Met – which remained consistent as a result of the different food intakes observed on diets varying in BCAA content. Supplementing only the metabolically essential AAs Trp or Thr, thereby rebalancing the diet for these AAs against BCAAs, significantly reduced hyperphagia associated with the BCAA200 diet. Indeed, exome matching predicted both Trp and Thr to be limiting in the BCAA200 diet, while Met is predicted to be over 3-fold in excess. Trp limitation in the imbalanced BCAA200 diet resulted in a downregulation of plasma metabolites associated with Trp metabolism including 5HT and 5-HIAA, a key neuropeptide and direct metabolite, derived solely from Trp and involved in energy balance and appetite control. Although studies have shown that suppressed thermogenesis in BAT of obese mice induced with a high fat diet is due to increased peripheral 5HT [51], the inverse relationship between peripheral BCAA and Trp in obese BCAA200 mice is likely due to direct manipulation of these AAs in the diet.

To elicit its effect on appetite regulation, Trp must cross the blood-brain-barrier for central 5HT synthesis, where it competes directly with the other large neutral AAs (LNAA) - phenylalanine, tyrosine and the BCAAs, for transport across the blood-brain barrier by the LAT1 AA transporter [24]. Indeed, reduced plasma ratios of Trp relative to the other LNAAs (‘tryptophan ratio’) have been associated with depression and obesity. Increased ingestion and circulating levels of BCAAs, as shown in BCAA200 mice, lowers brain Trp uptake and 5HT synthesis [52] as demonstrated by reduced plasma and cortex Trp: BCAA ratios in hyperphagic BCAA200 mice and reduced synaptic release of 5HT from the serotonergic neurons of the dorsal raphe nuclei. Early work in rats showed that peripheral injection of serotonergic agonists reduced food intake, while inhibition of 5HT activity restored feeding [53]. More recently, administration of selective serotonergic reuptake inhibitors (SSRIs), which increases serotonin availability, was reported to not only exert effects on mood and anxiety, but also reduce appetite [25]; a response we demonstrated by administering the SSRI fluoxetine to hyperphagic mice on a BCAA200 diet. We show, therefore, that hyperphagia in BCAA200 mice is linked to central Trp-mediated 5HT depletion, which is likely due to competition for LAT1 transport. An important next step will be to investigate the role of

LAT1 in mediating Trp uptake and serotonin production in our model of BCAA-mediated hyperphagia and obesity.

Several limitations of our study are acknowledged. First, our experiments did not directly measure BCAA turnover and metabolism and therefore the fate of excess dietary BCAAs, and whether they contribute directly to adiposity, remain unclear. Recent work using *in vivo* whole-body isotopic tracing show that in insulin resistant mice, there is a shift in BCAA oxidation from liver and adipose tissue towards muscle [54]. Therefore, it will be important for future studies to determine if BCAA oxidation and perturbations to AA homeostasis contribute to obesity in BCAA200 mice and whether AA uptake from circulation, protein turnover or AA oxidation differs in this mouse model.

Second, experimental diets used in this study were derived from a combination of casein and individual amino acids. The availability of free amino acids can influence gastric emptying with potential secondary affects mediated by activating vagal-vagal, enteroendocrine and enteric nervous systems and can also impact the rate of amino acids appearing in the blood stream [55,56]. Although using a combination of casein and free amino acids allowed precise manipulation of protein quality, future studies examining AA balance could consider the use of whole proteins to ensure normal physiological responses.

Third, we did not directly test palatability of our diets and amino acid manipulations may influence palatability, food intake and weight gain. Although palatability is important in acute feeding studies, issues around palatability are less relevant to explaining our results over long-term feeding. In insects [1] and mice [57], short-term palatability responses are typically overridden by prolonged exposure to a single diet, such that an initially unpalatable diet may ultimately be eaten in greater amounts than a more palatable one as animals compensate for nutritional deficiencies. In short, palatability is not fixed and a short-term assessment may not help explain long-term patterns of intake.

Finally, we acknowledge that the changes in hypothalamic gene expression and 5HT synaptic response in dorsal raphe neurons may be due to the balance of dietary BCAA: non-BCAAs or the hyperphagic nature of mice before tissue collection. To understand if there is a BCAA-specific effect, future investigations should provide the same diets, while controlling for energy intake. Any subsequent changes in gene expression or synaptic response can then be directly attributed to the dietary AA balance.

In conclusion, we show that long-term dietary BCAA manipulation influences healthspan and lifespan in mice by regulating food intake via a mechanism that involves their interaction with key non-BCAAs including Trp and Thr. Dietary amino acid imbalance influences central and peripheral appetite signaling via Trp-mediated 5HT depletion, resulting in hyperphagia, obesity, hepatosteatosis and reduced lifespan. These metabolic and lifespan costs occur in the absence of hepatic mTOR activation and are reversed by preventing hyperphagia using 20% CR or pair feeding. The results indicate that the adverse effects on an imbalanced high BCAA: non-BCAA diets are secondary to hyperphagia rather than any intrinsic BCAA toxicity. Food intake, health and lifespan are titrated against both the macronutrient composition, quantity and quality of dietary protein.

Europe PMC Funders Author Manuscripts

Methods

Animals and husbandry

BCAA longevity study—312 male and female C57BL/6J mice were obtained from the Australian Resource Centre (WA, Australia) at 4w old and housed at the Charles Perkins Centre at the University of Sydney under a 12 hour light: dark cycle. Experiments using C57BL/6J mice were conducted under the approval of Sydney University's Animal Ethics Committee: protocol 2014/752. Animals were housed four per cage in standard approved cages and were not exercised for the duration of the study (see Reporting Summary for additional details of animals and study design). At 12 weeks of age, mice were allocated to one of four experimental *ad libitum* (AL) diet treatments. An additional 192 male and female mice were obtained and assigned to 20% CR of either a BCAA100 or BCAA200 diet. Daily aliquots were estimated from the AL intake of the BCAA100 mice. Food intake and body weights were measured fortnightly until 6 months of age, followed by monthly measurements thereafter. Mice were checked twice weekly and animals losing more than 15% body weight were culled. At 15 months of age, plasma and tissue were collected from one mouse from each cage. Animals were anaesthetized using a mixture of ketamine and xylazine (100mg/kg ketamine and 16mg/kg xylazine) and euthanized by exsanguination via cardiac bleed using a 23G needle. Tissues harvested were snap frozen in liquid nitrogen or fixed for histology and included liver, muscle, white and brown fat, spleen, pancreas, kidneys, heart and reproductive organs. Tissue harvesting was performed between 10am and 12pm consistently, four to six hours after the initiation of the light cycle and when animals had completed their normal overnight feeding period. The rationale behind this collection time was to provide a stable, postprandial sample, several hours after the animals had completed their normal overnight feeding period. The collection time ensures that significant alterations to the normal diurnal pattern of feeding/fasting, active/sleeping are not introduced. This provides the best indication of their baseline response to the dietary interventions over 15 months of feeding, whereas overnight fasting introduces a significant fasting response in mice that would interfere with the normal hormonal and metabolite plasma profile due to innate nocturnal feeding patterns.

Short-term (6 week) dietary interventions—For short-term feeding experiments adding back Met, Thr or Trp to a BCAA200 diet (Fig. 2), 60 male C57BL/6J mice obtained from the Australian Resource Centre, housed two per cage at 12 weeks of age, were fed for 6 weeks on either a BCAA100, BCAA200, BCAA200+Trp, BCAA200+Thr or BCAA200+Met diet (see Supplemental tables 1 and 2 for detailed breakdown). Food intake was measured every 2 days and body weights recorded weekly. For studies investigating the effect of diet on serotonin (5HT) and Fluoxetine administration on food intake (Fig. 3), an additional 52, 6-week old male C57BL/6J mice from the Australian Resource Centre were purchased, housed 2 or 3 per cage and fed on either BCAA200 or BCAA100 diet for six weeks. Electrophysiological experiments were conducted on five mice/diet. The remaining 42 mice were treated with either Fluoxetine (n=24 mice; 8 cages) or saline (n=18 mice; 7 cages). All C57BL/6J mice were housed at the Charles Perkins Centre at the University of Sydney under a 12 hour light: dark cycle (Sydney University's Animal Ethics Committee: protocol 2014/752).

Exome-matching longevity study—C3B6F1 female hybrids were used for studies using exome-matched diets (Supplementary Table 4) and generated by a cross between C3H female and C57BL/6J male mice. Parental strains were obtained from Charles River Laboratories and experimental animals were bred in an in-house animal facility at the Max Planck Institute for Biology of Ageing, Germany. Four-week old female mice were housed in groups of five, in individually ventilated cages under specific-pathogen-free conditions. Experiments were conducted under the approval of the State Office for Nature, Environment and Consumer Protection North Rhine-Westphalia (Landesamt für Natur, Umwelt und Verbraucherschutz Nordrhein-Westfalen, LANUV), Germany, and the approval numbers are: 84-02.04.2012.A245 and 84-02.04.2017.A175.

Experimental diets

BCAA longevity study—All experimental diets, except for exome-matched diets, were custom designed and manufactured in dry, pelleted form by Specialty Feeds (WA, Australia). Diets were isocaloric (14.4 kJ/g) and matched in the total calculated net metabolizable energy from protein (18%) carbohydrate (64%) and fat (18%) (Supplementary Table 1). BCAA200: twice BCAA content of control diet AIN93G; BCAA100: standard content of BCAAs; and BCAA50 and BCAA20: containing one half and one fifth of standard content of BCAAs, respectively.

Short-term amino acid study—Diets with the addition of Thr, Trp or Met to a BCAA200 diet were matched for total energy content, BCAA content and macronutrient composition (Supplementary Table 2).

Exome-matching longevity study—Four week old C3B6F1 female hybrid mice were fed a 6% protein diet (AL) for three months. At the age of 4 months, mice were assigned one of three experimental diets and fed AL for 3 weeks, during which food intake was recorded 2 times per week. Groups with lowest food intake (23% protein, P23) was taken as the baseline group to which other groups were pair fed. Pair-feeding was done by measuring the food intake of mice fed P23 diet with AL access to food and adjusting the food intake of the rest of the mice accordingly. Food intake of control mice was measured twice a week and average value per week was used to adjust the food intake for the rest of the mice for the following week. Food aliquots were prepared one week in advance and all mice were fed daily at 9am. To minimize the differences in daily rhythms of feeding and activity between the control group and the rest of the groups, controls were also given daily aliquots of food which exceeded the amount normally eaten by this group.

To generate the theoretical requirement of mice for dietary amino acids, we used an *in silico* technique called exome matching [23]. Briefly, we used the complete set of protein coding sequences in the mouse genome (Ensembl v54 (May 2009, downloaded July 2, 2009)) to calculate the median proportional representation of each amino acid across all proteins. To determine the theoretically limiting amino acid, we divide the proportional representation of each dietary essential amino acid (expressed in moles) by its proportional representation in the mouse exome and find the amino acid with the lowest value. Every other amino acid is then considered to be in excess. For each mole of cysteine or tyrosine that was considered

undersupplied in the food the availability of methionine (for cysteine) or phenylalanine (for tyrosine) was reduced by one mole. The non-essential amino acids are not considered because they can be generated *de novo* as long as the general supply of nitrogen from other amino acids is sufficient. Exome matched diets used in the lifespan study and were manufactured by SSniff and were isocaloric (16.6 kJ/g, Supplementary Table 6). All amino acids were crystalline. 35-40% of BCAAs were added to the P6 diet (P6+BCAA) and all other amino acids were reduced to accommodate for BCAA supplementation.

Body composition

Body composition of C57BL/6J male and female mice was assessed using an EchoMRI 900 (EchoMRI, TX, USA) at 15 m of age. Additionally, Dual-energy x-ray absorptiometry (DEXA) scans were obtained using the Faxitron Ultrafocus 100 DXA (Faxitron, AZ) prior to tissue collection at 15 m. Animals were anaesthetized using 3% isoflurane and maintained at 1.5% and imaged. The region of interest was set to exclude the head and tail during scanning. Body composition of C3B6F1 female mice on exome-matched diets were measured with Minispec LF50H Body Analyzer (Bruker, Germany) at 12 m of age.

Glucose metabolism

Glucose tolerance tests were performed on C57BL/6J male and female at 15 m of age, by fasting mice for 4 h prior to testing. Basal blood samples were obtained by tail tipping and blood glucose measured using a clinical glucometer (Accu-Chek Performa, Roche Diagnostics Australia Pty Ltd). Glucose (2g kg^{-1} lean mass) was then administered via oral gavage. Blood was collected at baseline, 15, 30, 45, 60 and 90 minutes from the original tail wound and serial tail tipping was not required. The incremental area under the curve (AUC) was calculated. The AUC indicates the time taken to clear a bolus dose of glucose from the bloodstream and return to basal levels.

Metabolic hormones

FGF21 was measured in plasma collected from 15 m C57BL/6J male and female mice using the mouse/rat FGF21 ELISA kit as per manufacturer's protocols (Biovendor, Czech Republic). Mouse leptin, insulin and IGF-1 were also measured by ELISA, following the manufacturer's instructions (Crystal Chem IL).

Plasma amino acids

Amino acids from C57BL/6J male and female 15 m old mice were analyzed at the Australian Proteome Analysis Facility, Macquarie University, using the Waters AccQ-Tag Ultra Chemistry Kit (Waters Corporation).

Liver histology and triglyceride content

Paraffin embedded liver tissue collected from 15 m C57BL/6J male and female mice was sectioned at 5μm and stained with hematoxylin and eosin. The extent of steatosis and inflammation was assessed and scored (0 = 0% fat present, 1= 1-33%, 2= 34-66% and 3= >67%) by four independent observers blinded to the dietary treatment groups.

Liver triglyceride content was measured by homogenizing 30mg of frozen tissue from C57BL/6J male and female 15 m mice in a 1:2 ratio of methanol and chloroform using a bead-based tissue lyser. Lipids were extracted overnight on a roller and dried down using a nitrogen apparatus and a heating block at 37°C-45°C. Dried sample was then resuspended in absolute ethanol (RNA grade), quantified by GPO-PAP method (Catalogue no. TG1730711; Roche) with absorbance measured using a Tecan Infinite M1000 PRO plate reader at 490nm.

Blood lipids and biochemistry

Blood cholesterol, triglycerides, liver function tests (alanine transaminase, ALT and aspartate amino transferase, AST) analysis were performed on plasma collected from C57BL/6J male and female 15 m mice at the Diagnostic Pathology Unit, Concord Hospital, NSW Health using a Cobas 8000, c702 photometric module (Hitachi, Japan).

Metabolic phenotyping

To determine whole-animal metabolic rate, substrate utilization and activity, 12-16 C57BL/6J male and female mice per diet were housed individually and assessed by indirect calorimetry in a Promethion high-definition behavioral and continuous respirometry system for mice (Sable Systems International, NV, USA) at 15 m of age. Oxygen consumption (VO2) and carbon dioxide production (VCO2) were measured over 48 hours, following an 8 hour acclimation period, and maintained at ~22°C under a 12:12 hour light: dark cycle. Energy expenditure is shown a kcal/h corrected for lean mass. Mice were not given access to a running wheel.

Electrophysiology

Following six weeks on either a BCAA200 or BCAA100 diet, coronal dorsal raphe brain slices (280 μM) from 12 w old C57BL/6J male mice were cut using the Leica VT 1200s vibratome. Slices were initially incubated in recovery solution containing (in mM) 93 NMDG chloride, 2.5 KCl, 1.2 NaH_2PO_4, 30 $NaHCO_3$, 20 HEPES, 25 D-Glucose, 5 sodium ascorbate, 2 thiourea, 3 sodium pyruvate, 10 $MgCl_2$, 0.5 $CaCl_2$, pH 7.3, 300-310 mOsm/L heated at 34°C and saturated with carbogen for 10 minutes and then stored in physiological saline (ACSF) for at least 1 hr either with or without the addition of tryptophan (50 μM). Slices were transferred to a recording chamber and superfused continuously at 2.5ml/min with 34°C ACSF containing (in mM) 125 NaCl, 2.5 KCl, 1.25 $NaH_2PO_4.2H_2O$, 1 $MgCl_2$, 2 $CaCl_2$, 25 $NaHCO_3$ and 11 D-Glucose saturated with carbogen. Dorsal raphe neurons were visualized using an Olympus BX51 microscope using Dodt gradient contrast optics. Whole cell patch-clamp recordings were made from dorsal raphe neurons using internal solution containing 95 mM potassium gluconate, 30 mM KCl, 10 mM HEPES, 2 mM EGTA, 15 mM NaCl, 1 mM $MgCl_2$, 2 mM MgATP and 0.3 mM NaGTP. Neurons were voltage clamped at −60 mV and liquid junction potentials of −12 mV were not corrected. Electrically evoked IPSCs were elicited via bipolar tungsten stimulating electrodes (10 stimuli delivered at 166 Hz, 100 V, 100 μs). Membrane currents were recorded using Multiclamp 700B amplifier (Molecular Devices), digitized and then acquired and analyzed using Axograph Acquisition software (Molecular Devices). All recordings were made in the presence of 100 μM picrotoxin (Sigma-Aldrich), 50 μM DL-2-amino-5-phosphonopentanoic acid (DL-APV, (Abcam, Cambridge UK)), 500 nM prazosin (Sigma-Aldrich), 10 μM CNQX (Abcam) and 1

μM CGP 55845 (Tocris). Stock solutions of drugs were made in distilled water except for NAN-190 (Sigma-Aldrich), which was dissolved in DMSO, and then diluted to their final concentration in ACSF and applied by superfusion.

Fluoxetine administration

Following six weeks on a BCAA200 diet, 12 w old male C57BL/6J mice were gavaged with either Fluoxetine (20 mg/kg; Selleckchem TX, USA) or saline for four days. Food intake was recorded daily.

Gene expression

Total RNA from C57BL/6J 15 m male and female liver and hypothalamus were extracted using the Trizol method (Sigma) and quantified spectrophotometrically using a NanoDrop (Thermo Scientific). For RNAseq, hypothalamic RNA was sequenced by the Australian Genome Research Facility (AGRF Ltd) using Illumina HiSeq 2500. The sequence reads were analyzed according to AGRF quality control measures. The cleaned sequence reads were then aligned against the *Mus musculus* genome (GRCm38). The Tophat aligner (v2.0.14) was used to map reads to the genomic sequences. The transcripts were assembled with the Stringtie tool v1.2.4 utilizing the reads alignment with gencode M14. The Fragments Per Kilobase of transcript per Million mapped reads (FPKM) were generated using Stringtie based on the formula: $FPKM=10_6\ C\ /\ (NL/10_3)$, C is number of reads that uniquely aligned to a gene, N is total number of reads that uniquely aligned to all genes, and L is number of bases of a gene. Heatmaps were generated to model the relationship of BCAA intake with gene expression as measured by standardized Z-scores. The rows are organized by hierarchical clustering using agglomerative clustering with complete linkage and Euclidian distance metric.

For real-time PCR, cDNA was synthesized (BioRad iScript) and mRNA expression analyzed using SYBR green methodology (LightCycler 480, Roche). Primer pairs were designed using the Roche Universal Probe Library and BLASTed against the NCBI mouse genomic sequence database. Reactions were performed in triplicate and target gene expression normalized with eef2 as the endogenous control. Fold-change (FC) was calculated based on a pooled sample. Primers were 300nM in concentration and sequences for each gene are described: *Npy*–F CGACACTACATCAATCTCATC, *Npy*–R AAGTTTCATTTCCCATCACC; *Agrp*–F CTTCTTCAATGCCTTTTGC, *Agrp*–R TTTTTAAACCGTCCCATCC; *Lepr*–F TGCTGAATTATACGTGATCG, *Lepr*–R AGACGTAGGATGAATAGATGG; *Socs3*–F ATTTCGCTTCGGGACTAGC, *Socs3*-R AACTTGCTGTGGGTGACCAT; *Pepck*–F CCAACGTGGCCGAGACTAGCG, *Pepck*–R GGCACATGGTTCCGCGTCCT; *Eef2*–F TGTCAGTCATCGCCCATGTG, *Eef2*–R CATCCTTGCGAGTGTCAGTGA; *Fgfr1c*–F TCCTCTTCTGGGTGTGC, *Fgfr1c*–R CTCCACTTCCACAGGGACTC; *Klb*–F GAGGATGATCAGATCCGAAAGT, *Klb*–R AGCCTTTGATTTTGACCTTGTC.

Protein quantification

For all western blots, protein concentration was determined with a BCA assay (Sigma) and lysates loaded and standardized to contain 25 μg of protein. Liver, white adipose tissue and

brown adipose tissue from 15 m old C57BL/6J male and female mice were resolved in a either a 4-12% Bis-Tris gel (BioRad) or 3-7% Tris-Acetate gel (BioRad). Following electrophoresis, proteins were transferred to a nitrocellulose membrane, blocked with 5% BSA in TBST and incubated with various primary antibodies (mTOR, Cell Signaling 2972; phospho-mTOR (Ser 2448), Cell Signaling 2971; UCP1, Cell Signaling 04670; ACLY, Cell Signaling 13390; SCD1, Cell Signaling 2438; FASN, Cell Signaling 3180; ACC, Cell Signaling 3662; β-actin, Cell Signaling 13E5; cyclophilin, Cell Signaling 2175 (see Reporting Summary)) overnight at 4°C. Bands were imaged following incubation for 1h at room temperature in anti-rabbit HRP-linked secondary antibody (Cell Signaling 7404) on a ChemiDoc (BioRad) using ImageLab software to quantify relative protein expression.

Metabolomics

Targeted LC-QQQ-MS analysis was performed to detect a different set of water soluble metabolites in the positive and negative ionizations mode were conducted using an LC-MS system comprised of an Agilent 1260 Infinity liquid chromatography coupled to a QTRAP 5500 mass spectrometer (AB SCIEX). Samples for analysis were from C57BL/6J 15 m male and female mice. HILIC Method: Plasma and cortex samples (10 μL) were prepared via protein precipitation with the addition of nine volumes of 74.9:24.9:0.2 v/v/v acetonitrile/methanol/formic acid containing stable isotope-labeled internal standards (valine-d8 (Sigma-Aldrich), and phenylalanine-d8 (Cambridge Isotope Laboratories)). Amide Method: Plasma samples (30 μL) were prepared via protein precipitation with the addition of 70 μL of 75:25 v/v of acetonitrile/methanol containing stable isotope-labeled internal standards (Thymine-d4 (Sigma-Aldrich), and phenylalanine-d8 (Cambridge Isotope Laboratories)). The samples were centrifuged (20 min, 14 000 rpm, 4°C), and the supernatants (10 μL) were injected directly onto a 2.1 x 150 mm, 3 μm Atlantis HILIC column (Waters; Milford, MA) and a 4.6 x 100mm, 3.5μm XBridge Amide, for HILIC and Amide analysis, respectively. 80 metabolites from the 84 metabolites optimized for positive mode detection were detectable in the plasma extracts. Of 110 metabolites optimized for negative mode, 73 were detectable in the mice plasma and included in the final MRM method. Raw data files (Analyst software, version 1.6.2; AB Sciex, Foster City, CA, USA) were imported into the provided analysis software Multi-Quant 3.0 for MRM Q1/Q3 peak integration and data were normalized relative to pooled plasma samples that were analyzed in the sample queue after every 10 study samples.

Immunohistochemistry and islet analysis

Paraffin-embedded pancreas from 15 m C57BL/6J male and female mice were sectioned and then stained as follows; sections were deparaffinized and rehydrated through a xylene-ethanol series and washed twice in PBS containing 0.1% BSA and 0.01% sodium azide (Wash Buffer). Slides were incubated with Blocking Buffer (DAKO) for 1h at RT, then incubated with guinea pig anti-insulin (DAKO, A0564) and mouse anti-glucagon (Sigma, G2654) overnight at 4 °C in a humidified chamber (see Reporting Summary for antibody details). The following day, slides were washed twice in Wash Buffer, incubated in goat anti-guinea pig igG and donkey anti-mouse igG secondary antibodies (Life Technologies, 488 and 594, respectively), washed twice again and then mounted in Prolong Diamond Antifade

Europe PMC Funders Author Manuscripts

Mountant containing DAPI (Thermo Fisher Scientific). Slides were imaged with Leica DM6000 wide field and SP8 confocal microscopes.

Images were analyzed using FIJI Image J (v1.52b). Total pancreas area was calculated by tile-stitching entire pancreas sections in each slide. Fluorescence intensity after threshold of anti-insulin and anti-glucagon staining were used to calculate total insulin and glucagon positive area respectively, and total islet area was measured as a sum of total insulin and glucagon staining. At least 10 islets per pancreas were averaged to obtain each individual mouse pancreas measurement.

Statistical analyses

Data are presented as mean ± SEM and significance determined when $p < 0.05$ using *R* (v3.4.1) and Graphpad Prism (v7.02). Comparisons between dietary treatments on various responses were analyzed with ANOVA and non-parametric data was analyzed with Kruskal Wallis test. Sex was added as a cofactor and responses showing a significant diet*sex interaction are shown in Supplementary Fig. 3 and Supplementary Table 5. Comparisons of metabolic responses between AL and CR animals were performed using unpaired t-test (two-sided). Details of statistical tests for each graph are described in each figure legend. See Reporting Summary for data analysis and software specifications.

Survival data for C57BL/6J male and female mice and C3B6F1 female mice were analyzed in the *survival* package in *R* using Cox proportional hazards models (CPHMs) implemented using the 'coxph' function (R development Core Team (2008)) [59,60]. CPHMs were used as they allowed us to explore interactions between diet and sex effects on survival, as well as, where required, time-dependent effects in expanded CPHMs. Including additive or interactive effects of sex alongside diet did not improve model fits based on AIC (BCAA data, Fig. 1n, $AIC_{Diet} = 1935.9$, $AIC_{Diet+Sex} = 1935.7$, $AIC_{Diet*Sex} = 1936$; CR data, Fig. 7a, $AIC_{Diet} = 2075.6$, $AIC_{Diet+Sex} = 2075.6$, $AIC_{Diet*Sex} = 2076.2$) suggesting diet alone is the best predictor of survival in the experiments.

For BCAA data from C57BL/6J male and female mice (Fig. 1n), we explored an expanded time-dependent CPHM (survival curves cross around week 60), however this model detected no significant interaction between time (pre- *vs* post week 60) and diet (CPHM BCAA*Time Est = 0.95, SE = 0.94, $p = 0.31$). CPHM detected significant differences in survival between animals on BCAA200, and all other diets (BCAA20 vs BCAA200 Est. = -0.58, SE = 0.21, $p < 0.005$; BCAA50 vs BCAA200 Est. = - 0.48, SE = 0.20, $p < 0.05$; BCAA100 vs BCAA200 Est. = -0.49, SE = 0.19, $p < 0.005$). It should be noted that ten BCAA20 animals were euthanized before 60 weeks of age because of weight loss (n=5) or seizures (n=5) and these were excluded from the survival analysis. For data comparing AL and CR-fed mice (Fig. 7a), significant differences were detected (Cox proportional hazards modelling: CR *vs* AL $p < 0.001$; 100 *vs* 200 AL $p=0.01$; 100 *vs* 200 CR $p=0.68$). For exome-matched feeding experiments using C3B6F1 female mice, we found CPHM detected significant differences in survival on P23 diets relative to P6 (Est. 0.68, SE = 0.21, $p < 0.005$), but not between P6 and P6+BCAA (Est. = -0.24, SE = 0.23, p = 0.30).

Metabolites from C57BL/6J male and female 15 m old mice were correlated with BCAA intake and those with a Pearson correlation coefficient (r) >0.1 were analyzed in Metaboanalyst using the KEGG (*Mus musculus*) pathway library (v4.0; https://www.metaboanalyst.ca/faces/home.xhtml) [61–63]. Both positively and negatively correlated metabolite sets were analyzed using the integrated pathway analysis and significant Holm adjusted p-values are plotted in Fig. 3.

For hypothalamic data from male and female C57BL/6J 15 m old mice analyzed by RNAseq, correlation coefficients of BCAA intake and the FPKM value of each gene were plotted as heatmaps, and show genes with a significant p-value. For volcano plots, the FPKM data were filtered with averaged FPKM for each gene greater than 0.1. The Pearson correlation coefficient and corresponding p-value for each gene were calculated. Correlation coefficients with less than 0.5th percentile or greater than 99.5th percentile was considered as significant and marked with red-dashed lines. FPKM data were correlated with BCAA intake and genes with moderate to strong correlation (r >0.3) were analyzed in the Database for Annotation, Visualization and Integrated Discovery (DAVID) (v6.8; https://david.ncifcrf.gov/home.jsp) [29,64]. Both positively and negatively correlated gene sets were analyzed using the Functional Annotation Tool and pathways assessed using the KEGG (*Mus musculus*) pathway library and shown in Supplementary Table 4.

Supplementary Material

Refer to Web version on PubMed Central for supplementary material.

Acknowledgements

We thank F. Held and P. Telleria Teixeira for their technical and administrative support. We thank Laboratory Animal Services at the University of Sydney, N. Sunn of Sydney Imaging, W. Potts from Specialty Feeds, L. McQuade from the Australian Proteome Analysis Facility and the Diagnostic Pathology Unit at Concord Hospital. This work is supported by NHMRC project grant (GNT1084267 and GNT571328 to DR, DLC and SJS), the Ageing and Alzheimers Institute and the Sydney Food and Nutrition Network. SSB is supported by the NHMRC Peter Doherty Biomedical Fellowship (GNT1110098) and the University of Sydney SOAR fellowship. AMS was supported by the Australian Research Council. VCC is supported by a University of Sydney Equity Fellowship. LP and PJ were supported by the Max Planck Society and acknowledge funding from the European Research Council under the European Union's Seventh Framework Programme (FP7/2007-2013) / ERC grant agreement 268739 and the Wellcome Trust.

References

1. Simpson, SJ, Raubenheimer, D. The Nature of Nutrition A Unifying Framework From Animal Adaption to Human Obesity. Princeton University Press; 2012.
2. Gosby AK, et al. Testing Protein Leverage in Lean Humans: A Randomised Controlled Experimental Study. PLoS One. 2011; 6:e25929. [PubMed: 22022472]
3. Simpson SJ, Raubenheimer D. Obesity: The protein leverage hypothesis. Obesity Rev. 2005; 6:133–142.
4. Le Couteur DG, et al. The impact of low-protein high-carbohydrate diets on aging and lifespan. Cell Mol Life Sci. 2015; 76:1237–1252.
5. Solon-Biet SM, et al. The Ratio of Macronutrients, Not Caloric Intake, Dictates Cardiometabolic Health, Aging, and Longevity in Ad Libitum-Fed Mice. Cell Metab. 2014; 19:418–430. [PubMed: 24606899]
6. Solon-Biet SM, et al. Macronutrient balance, reproductive function, and lifespan in aging mice. Proc Natl Acad Sci USA. 2015; 112:3481–3486. [PubMed: 25733862]

7. Wahl D, et al. Comparing the Effects of Low-Protein and High-Carbohydrate Diets and Caloric Restriction on Brain Aging in Mice. Cell Rep. 2018; 25:2234–2243.e2236. [PubMed: 30463018]
8. Grandison RC, Piper MD, Partridge L. Amino-acid imbalance explains extension of lifespan by dietary restriction in Drosophila. Nature. 2009; 462:1061–1064. [PubMed: 19956092]
9. Miller RA, et al. Methionine-deficient diet extends mouse lifespan, slows immune and lens aging, alters glucose, T4, IGF-I and insulin levels, and increases hepatocyte MIF levels and stress resistance. Aging Cell. 2005; 4:119–125. [PubMed: 15924568]
10. Harper AE, Rogers QR. Amino acid imbalance. Proc Nutr Soc. 1965; 24:173–190. [PubMed: 5319199]
11. Hasek BE, et al. Dietary methionine restriction enhances metabolic flexibility and increases uncoupled respiration in both fed and fasted states. Am J Physiol. 2010; 299:R728–R739.
12. Soultoukis GA, Partridge L. Dietary Protein, Metabolism, and Aging. Annu Rev Biochem. 2016; 85:5–34. [PubMed: 27145842]
13. Fontana L, et al. Decreased Consumption of Branched-Chain Amino Acids Improves Metabolic Health. Cell Rep. 2016; 16:520–530. [PubMed: 27346343]
14. Newgard CB, et al. A Branched-Chain Amino Acid-Related Metabolic Signature that Differentiates Obese and Lean Humans and Contributes to Insulin Resistance. Cell Metab. 2009; 9:311–326. [PubMed: 19356713]
15. Maida A, et al. Repletion of branched chain amino acids reverses mTORC1 signaling but not improved metabolism during dietary protein dilution. Mol Metab. 2017; 6:873–881. [PubMed: 28752051]
16. She P, et al. Obesity-related elevations in plasma leucine are associated with alterations in enzymes involved in branched-chain amino acid metabolism. Am J Physiol Endocrinol Metab. 2007; 293:E1552–1563. [PubMed: 17925455]
17. Lackey DE, et al. Regulation of adipose branched-chain amino acid catabolism enzyme expression and cross-adipose amino acid flux in human obesity. Am J Physiol Endocrinol Metab. 2013; 304:E1175–1187. [PubMed: 23512805]
18. Piccolo BD, et al. Whey protein supplementation does not alter plasma branched-chained amino acid profiles but results in unique metabolomics patterns in obese women enrolled in an 8-week weight loss trial. J Nutr. 2015; 145:691–700. [PubMed: 25833773]
19. Fiehn O, et al. Plasma metabolomic profiles reflective of glucose homeostasis in non-diabetic and type 2 diabetic obese African-American women. PLoS ONE. 2010; 5:e15234. [PubMed: 21170321]
20. Huffman KM, et al. Relationships between circulating metabolic intermediates and insulin action in overweight to obese, inactive men and women. Diabetes Care. 2009; 32:1678–1683. [PubMed: 19502541]
21. Rose WC. II. The sequence of events leading to the establishment of the amino acid needs of man. Am J Public Health Nations Health. 1968; 58:2020–2027. [PubMed: 5748871]
22. Reeds PJ. Dispensable and Indispensable Amino Acids for Humans. J Nutr. 2000; 130:1835S–1840S. [PubMed: 10867060]
23. Piper MDW, et al. Matching Dietary Amino Acid Balance to the In Silico-Translated Exome Optimizes Growth and Reproduction without Cost to Lifespan. Cell Metab. 2017; 25:1206.
24. Breum L, Rasmussen MH, Hilsted J, Fernstrom JD. Twenty-four-hour plasma tryptophan concentrations and ratios are below normal in obese subjects and are not normalized by substantial weight reduction. Am J Clin Nutr. 2003; 77:1112–1118. [PubMed: 12716660]
25. Halford JC, Harrold JA, Lawton CL, Blundell JE. Serotonin (5-HT) drugs: effects on appetite expression and use for the treatment of obesity. Curr Drug Targets. 2005; 6:201–213. [PubMed: 15777190]
26. Hong S-H, et al. Minibrain/Dyrk1a Regulates Food Intake through the Sir2-FOXO-sNPF/NPY Pathway in Drosophila and Mammals. PLoS Genet. 2012; 8:e1002857. [PubMed: 22876196]
27. Morton NM, et al. A Stratified Transcriptomics Analysis of Polygenic Fat and Lean Mouse Adipose Tissues Identifies Novel Candidate Obesity Genes. PLoS One. 2011; 6:e23944. [PubMed: 21915269]

28. Cai D, Liu T. Hypothalamic inflammation: a double-edged sword to nutritional diseases. Ann N York Acad Sci. 2011; 1243:E1–39.
29. Huang da W, Sherman BT, Lempicki RA. Systematic and integrative analysis of large gene lists using DAVID bioinformatics resources. Nat Protoc. 2009; 4:44–57. [PubMed: 19131956]
30. O'Sullivan JF, et al. Dimethylguanidino valeric acid is a marker of liver fat and predicts diabetes. J Clin Invest. 2017; 127:4394–4402. [PubMed: 29083323]
31. Green CR, et al. Branched-chain amino acid catabolism fuels adipocyte differentiation and lipogenesis. Nat Chem Biol. 2016; 12:15–21. [PubMed: 26571352]
32. White PJ, et al. The BCKDH Kinase and Phosphatase Integrate BCAA and Lipid Metabolism via Regulation of ATP-Citrate Lyase. Cell Metab. 2018; 27:1281–1293.e1287. [PubMed: 29779826]
33. Wang TJ, et al. Metabolite profiles and the risk of developing diabetes. Nat Med. 2011; 17:448–453. [PubMed: 21423183]
34. Shah SH, et al. Branched-chain amino acid levels are associated with improvement in insulin resistance with weight loss. Diabetologia. 2012; 55:321–330. [PubMed: 22065088]
35. Connelly MA, Wolak-Dinsmore J, Dullaart RPF. Branched Chain Amino Acids Are Associated with Insulin Resistance Independent of Leptin and Adiponectin in Subjects with Varying Degrees of Glucose Tolerance. Metab Syndr Relat Disord. 2017; 15:183–186. [PubMed: 28437198]
36. Zheng Y, et al. Cumulative consumption of branched-chain amino acids and incidence of type 2 diabetes. Int J Epidemiol. 2016; 45:1482–1492. [PubMed: 27413102]
37. Felig P, Marliss E, Cahill GF Jr. Plasma amino acid levels and insulin secretion in obesity. N Engl J Med. 1969; 281:811–816. [PubMed: 5809519]
38. Lake AD, et al. Branched chain amino acid metabolism profiles in progressive human nonalcoholic fatty liver disease. Amino acids. 2015; 47:603–615. [PubMed: 25534430]
39. Goffredo M, et al. A Branched-Chain Amino Acid-Related Metabolic Signature Characterizes Obese Adolescents with Non-Alcoholic Fatty Liver Disease. Nutrients. 2017; 9:642.
40. Isanejad M, et al. Branched-chain amino acid, meat intake and risk of type 2 diabetes in the Women's Health Initiative. Br J Nutr. 2017; 117:1523–1530. [PubMed: 28721839]
41. Elshorbagy AK, et al. Food Overconsumption in Healthy Adults Triggers Early and Sustained Increases in Serum Branched-Chain Amino Acids and Changes in Cysteine Linked to Fat Gain. J Nutr. 2018; 148:1073–1080. [PubMed: 29901727]
42. Stöckli J, et al. Metabolomic analysis of insulin resistance across different mouse strains and diets. J Biol Chem. 2017; 292:19135–19145. [PubMed: 28982973]
43. Gietzen DW, Hao S, Anthony TG. Mechanisms of food intake repression in indispensable amino acid deficiency. Annu Rev Nutr. 2007; 27:63–78. [PubMed: 17328672]
44. Rose WC. Feeding experiments with mixtures of highly purified amino acids I. The inadequacy of diets containing nineteen amino acids. J Biol Chem. 1931; 94:155–165.
45. Lynch CJ, Adams SH. Branched-chain amino acids in metabolic signalling and insulin resistance. Nat Rev Endocrinol. 2014; 10:723–736. [PubMed: 25287287]
46. Newgard CB. Interplay between lipids and branched-chain amino acids in development of insulin resistance. Cell Metab. 2012; 15:606–614. [PubMed: 22560213]
47. She P, et al. Disruption of BCATm in mice leads to increased energy expenditure associated with the activation of a futile protein turnover cycle. Cell Metab. 2007; 6:181–194. [PubMed: 17767905]
48. Zhang Y, et al. Increasing dietary leucine intake reduces diet-induced obesity and improves glucose and cholesterol metabolism in mice via multimechanisms. Diabetes. 2007; 56:1647–1654. [PubMed: 17360978]
49. Hiroshige K, Sonta T, Suda T, Kanegae K, Ohtani A. Oral supplementation of branched-chain amino acid improves nutritional status in elderly patients on chronic haemodialysis. Nephrol Dial Transplant. 2001; 16:1856–1862. [PubMed: 11522870]
50. D'Antona G, et al. Branched-Chain Amino Acid Supplementation Promotes Survival and Supports Cardiac and Skeletal Muscle Mitochondrial Biogenesis in Middle-Aged Mice. Cell Metab. 2010; 12:362–372. [PubMed: 20889128]

51. Crane JD, et al. Inhibiting peripheral serotonin synthesis reduces obesity and metabolic dysfunction by promoting brown adipose tissue thermogenesis. Nat Med. 2014; 21:166. [PubMed: 25485911]
52. Fernstrom JD. Branched-chain amino acids and brain function. J Nutr. 2005; 135:1539s–1546s. [PubMed: 15930466]
53. Gietzen DW, Rogers QR, Leung PM, Semon B, Piechota T. Serotonin and feeding responses of rats to amino acid imbalance: initial phase. Am J Physiol. 1987; 253:R763–771. [PubMed: 2446514]
54. Neinast MD, et al. Quantitative Analysis of the Whole-Body Metabolic Fate of Branched-Chain Amino Acids. Cell Metab. 2018
55. Dangin M, et al. The digestion rate of protein is an independent regulating factor of postprandial protein retention. Am J Physiol Endocrinol Metab. 2001; 280:E340–348. [PubMed: 11158939]
56. Taylor IL, Byrne WJ, Christie DL, Ament ME, Walsh JH. Effect of individual l-amino acids on gastric acid secretion and serum gastrin and pancreatic polypeptide release in humans. Gastroenterology. 1982; 83:273–278. [PubMed: 6806140]
57. Tordoff MG, Pearson JA, Ellis HT, Poole RL. Does eating good-tasting food influence body weight? Physiol Behav. 2017; 170:27–31. [PubMed: 27988248]
58. Therneau TM. A package for survival analysis in S v. 2.38. 2015
59. Therneau, TM, Grambsch, M. Modeling survival data: extending the cox model. Springer; 2000.
60. Therneau TM. A package for survival analysis in S. 2015
61. Chong J, et al. MetaboAnalyst 4.0: towards more transparent and integrative metabolomics analysis. Nucleic Acids Res. 2018; 46:W486–W494. [PubMed: 29762782]
62. Xia J, Wishart DS. Web-based inference of biological patterns, functions and pathways from metabolomic data using MetaboAnalyst. Nat Protoc. 2011; 6:743. [PubMed: 21637195]
63. Xia J, Wishart DS. Metabolomic Data Processing, Analysis, and Interpretation Using MetaboAnalyst. Curr Protoc Bioinformatics. 2011; 34:14.10.11–14.10.48.
64. Huang da W, Sherman BT, Lempicki RA. Bioinformatics enrichment tools: paths toward the comprehensive functional analysis of large gene lists. Nucleic Acids Res. 2009; 37:1–13. [PubMed: 19033363]

Europe PMC Funders Author Manuscripts

Europe PMC Funders Author Manuscripts

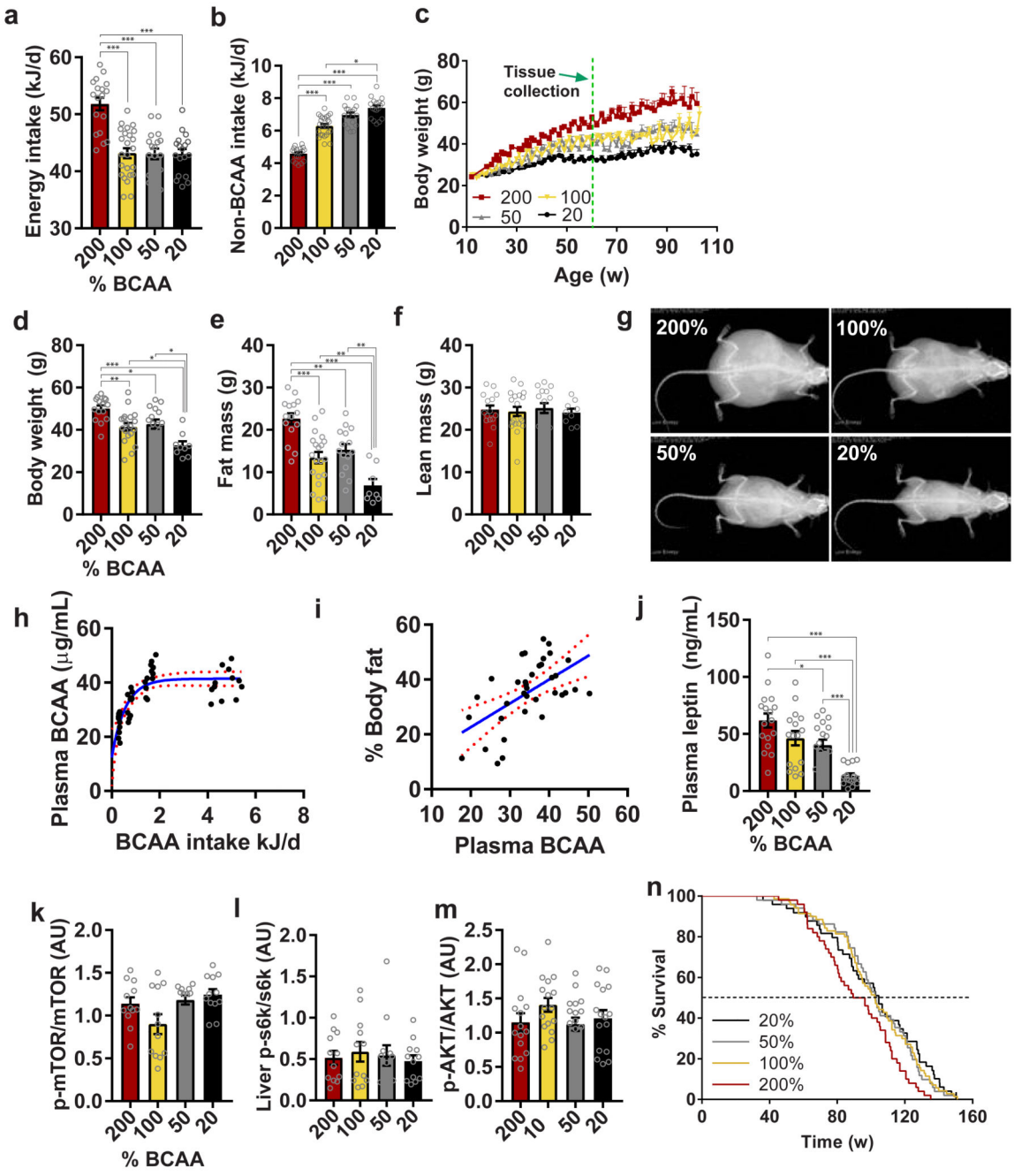

Fig. 1. Dietary BCAA imbalance drives hyperphagia, obesity and shortens lifespan

(a) Energy intake and (b) non-BCAA intake averaged over 12-15 months of age (200%, 50%, 20%, n=18; 100%, n=24 independent cages). (c) Body weight trajectories over time (200%, 50%, 20%, n=72; 100%, n=96 biologically independent mice). The green dashed line indicates the 15 month tissue collection time point from which plasma and tissue were analyzed. (d) body weight (200%, n=15; 100%, n=19; 50%, n=15; 20%, n=9 independent cages), (e) fat mass (200%, n=15; 100%, n=20; 50%, n=15; 20%, n=8 independent cages) and (f) lean mass (200%, n=15; 100%, n=19; 50%, n=15; 20%, n=9 independent cages)

measured longitudinally using EchoMRI. (g) Representative DEXA scans of mice measured once at 15 months of age (200%, n=9; 100%, n=8; 50%, n=11; 20%, n=10 biologically independent mice) (h) Plasma BCAAs vs BCAA intake from animals at collected at 15 months of age (n=47 biologically independent mice). (i) % body fat (r= 0.329, Pearson's correlation, p=0.0003) measured by EchoMRI vs plasma BCAAs at 15 months of age (n=47 biologically independent mice). Red lines show the 95% confidence interval. (j) Plasma leptin levels at 15 months of age (200%, n=17; 100% and 20%, n=16, 50%, n=18 biologically independent mice). (k-m) Hepatic mTOR (n=12 biologically independent mice for all groups), S6K (n=12 biologically independent mice for all groups) and AKT (200%, 100% and 20%, n=16; 50%, n=18 biologically independent mice) activation analyzed by western blot. (n) Survival curves analyzed by Cox Proportional Hazard Models (CPHM). Dotted line indicates median lifespan. Data shown are for combined sexes analyzed at 15 months of age. For all bar graphs, ANOVA was used for normal and log-normal data, and Kruskal Wallis for non-normal data. Pairwise comparisons amongst diets for normal and log-normal data were made using t-tests (two-sided). For non-normal data, pairwise comparisons amongst diets were made using Kruskal Wallis test. All bars indicate means ± SEM. *p≤0.05, **p≤0.01, ***p≤0.001 based on posthoc analysis following correction for multiple testing.

Europe PMC Funders Author Manuscripts

Europe PMC Funders Author Manuscripts

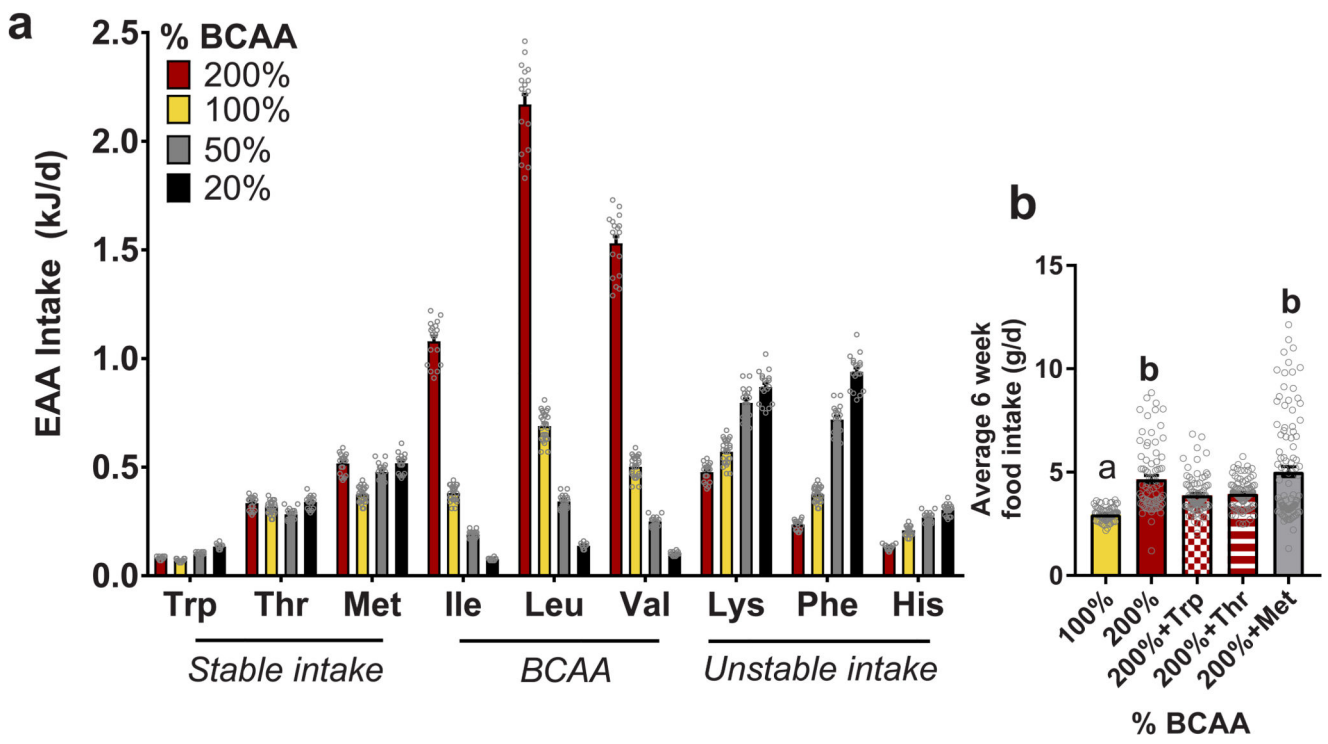

Fig. 2. Tryptophan and threonine supplementation prevents hyperphagia

(a) Average intake of essential amino acids (EAA) over 12-15 months (200%, 50% and 20%, n=18; 100%, n=24 biologically independent mice). AAs were categorized as those that remained stable in intake across diets, the BCAAs and those that were unstable across diets. The three AAs which remained stable (Trp, Thr and Met) were used in a six week feeding study. (b) Over six weeks of feeding, male mice on a BCAA200 diet were hyperphagic as seen in the long-term study. Adding back 150% of Trp or Thr significantly suppressed hyperphagia (100%, n=82; 200%, n=79; 200%+Thr, n=99; 200%+Trp, n=91; 200%+Met, n=105 independent daily measurements of food intake). For all bar graphs, ANOVA for normal and log-normal data, and Kruskal Wallis tests for non-normal data, were used to determine significant differences between groups. Pairwise comparisons amongst diets for normal and log-normal data were made using t-tests (two-sided). For non-normal data, pairwise comparisons amongst diets were made using Kruskal Wallis test. For (a), ANOVA was used for normal and log-normal data, and Kruskal Wallis for non-normal data. Pairwise comparisons amongst diets for normal and log-normal data were made using t-tests (two-sided). For non-normal data, pairwise comparisons amongst diets were made using Kruskal Wallis test. For (b), one-way ANOVA was performed with Tukey's multiple comparisons test. 100% vs 200%, $p<1x10^{-15}$; 100% vs 200%+Thr, $p=8.3x10^{-5}$, 100% vs 200%+Trp, $p=3.6x10^{-4}$; 100% vs 200%+Met, $p<1x10^{-15}$; 200% vs 200%+Thr, p=0.010; 200% vs 200% +Trp, p=0.005; 200%+Thr vs 200%+Met, $p=2.1x10^{-6}$; 200% Trp vs 200% Met, $p=9.5x10^{-7}$. All bars indicate means ± SEM and groups that do not share common letters indicate significant differences ($p<0.05$) based on posthoc analysis.

Europe PMC Funders Author Manuscripts

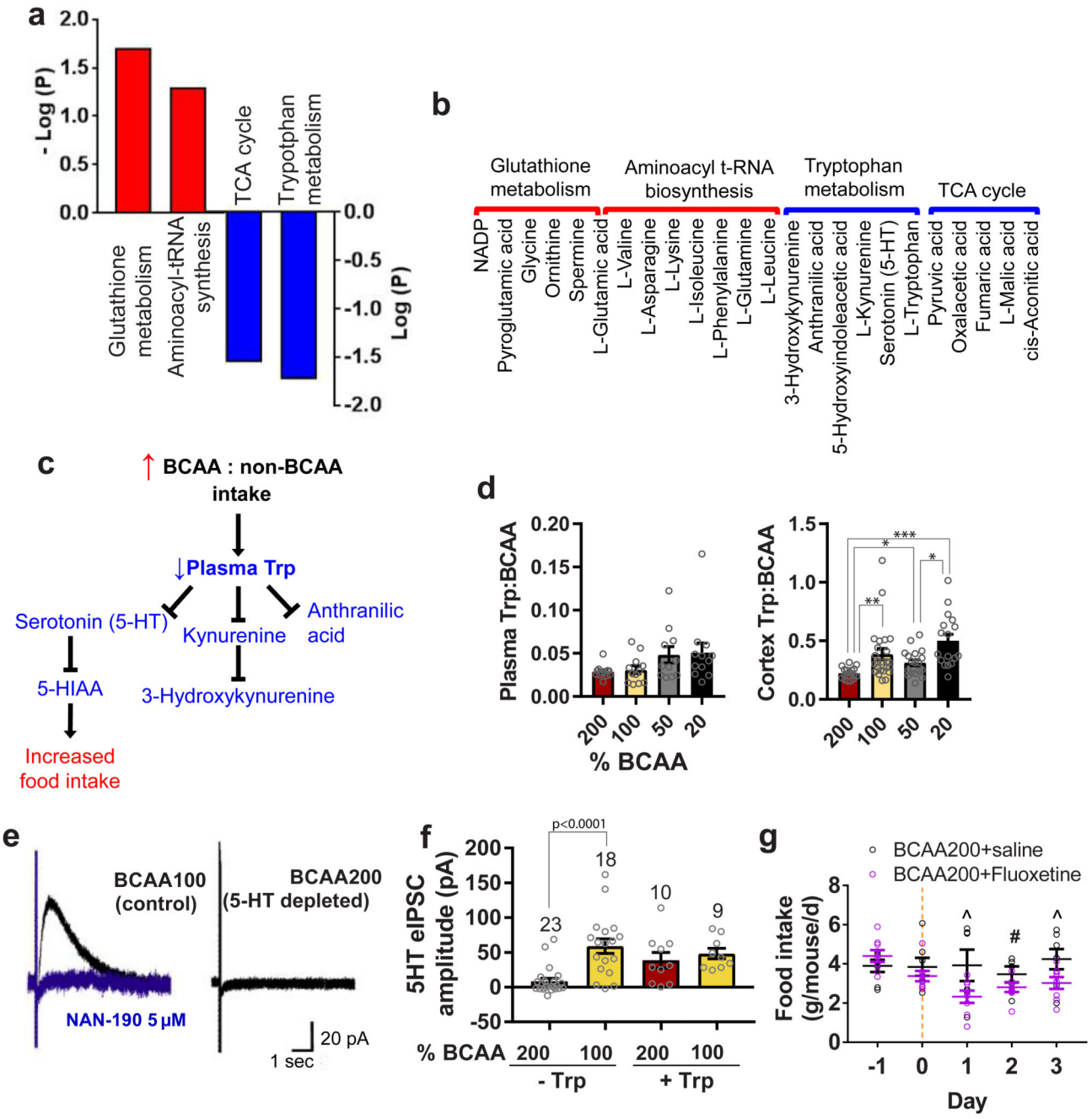

Fig. 3. Hyperphagia in BCAA200 mice is linked to Trp-mediated serotonin (5-HT) depletion

Metabolic pathways (KEGG) positively (red) and negatively (blue) correlated with high BCAA: non-BCAA intakes measured in plasma of 15 month old mice using LC-MS and the (b) metabolites in each pathway (200% and 50% n= 17; 100%, n=14; 20% n=16 biologically independent mice). (c) Diagram depicting the relationship between dietary BCAA:non-BCAA intake, Trp metabolism and the effects on food intake. (d) The ratio of Trp:BCAA in plasma and cortex of mice collected at 15 months of age (Plasma: 200%, 100% and 20%, n=12; 50%, n=11 biologically independent mice. Cortex: 200%, n=16; 100%, n=24; 50%,

n=18; 20%, n=17 biologically independent mice). (e) Example traces from electrophysiological patch clamp recordings showing 5HT synaptic responses from mice fed either the BCAA100 (control) or BCAA200 (predicted 5HT depleted) diet for six weeks (n=5 biologically independent mice). The evoked inhibitory post-synaptic current (eIPSC) is shown in black and blocking by the 5HT1A receptor antagonist NAN-190 in blue. (f) Average 5HT eIPSC amplitude without and with addition of Trp to media. Number of neurons measured are shown above bars. (g) Food intake of mice on BCAA200 diets following four days of oral administration of either fluoxetine or saline (saline, n=7; fluoxetine, n=8 independent cages). For (a,b) Pearson's correlation. In (d,e) data are from males and females combined. For (d), pairwise comparisons for normal and log-normal data were made using t-tests (two-sided). For non-normal data, pairwise comparisons amongst diets were made using Kruskal Wallis test. For (f), pair-wise comparisons were made between the 200% and 100% groups, without and with Trp, using t-tests (two-sided). In (g), ^ denotes a significant difference between treatments (Day 1, p=0.030; Day 3, p=0.028) and # indicates near significance (p=0.078) based on t-test (one-sided). All bars indicate means ± SEM. *p≤0.05, **p≤0.01, ***p≤0.001, unless otherwise shown, based on posthoc analysis following correction for multiple testing.

Europe PMC Funders Author Manuscripts

Europe PMC Funders Author Manuscripts

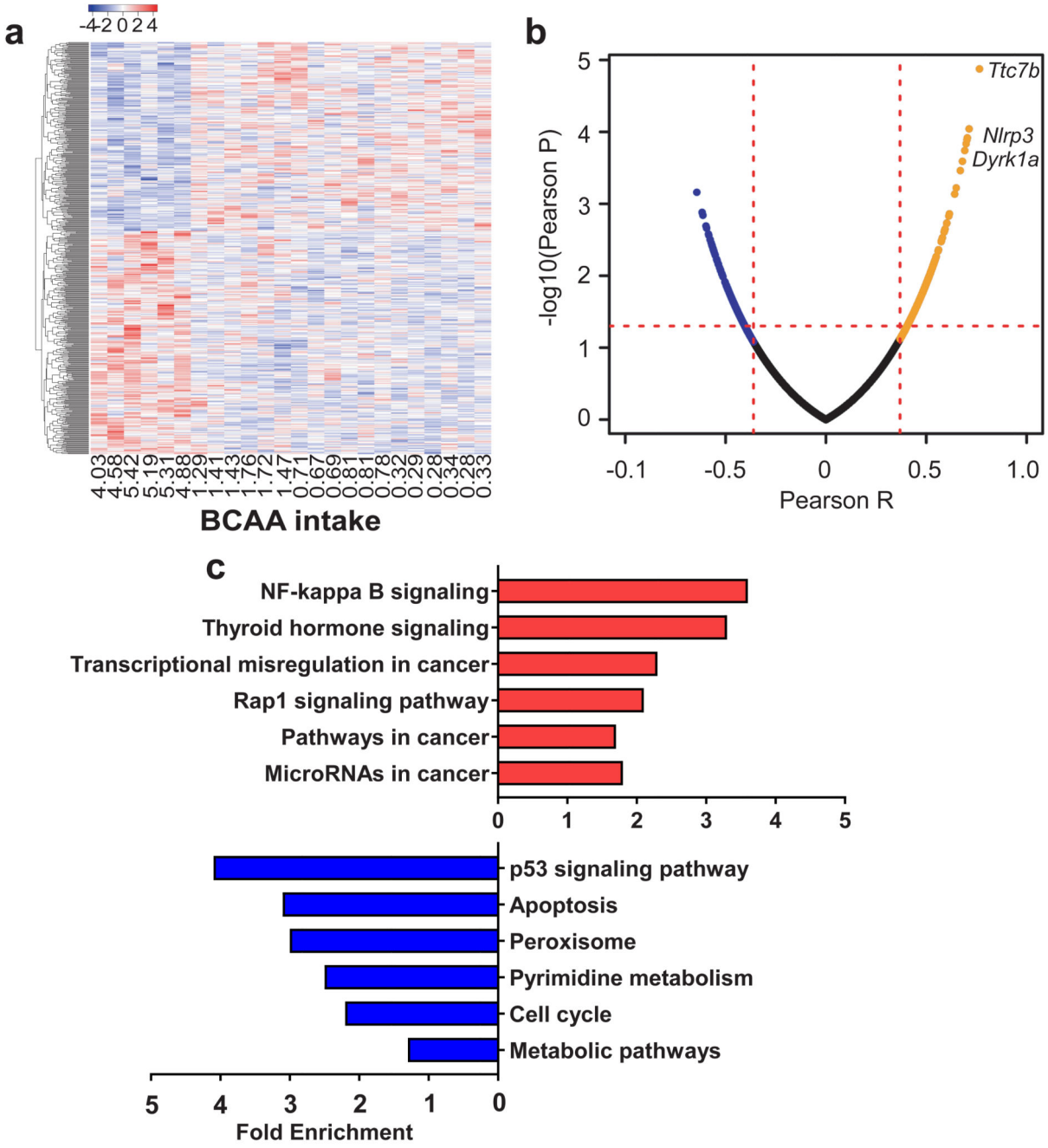

Fig. 4. The ratio of dietary BCAA to non-BCAAs influence hypothalamic gene expression

(a) Heatmap of hypothalamic genes significantly correlated with BCAA intake (averaged over 12-15 months of age) measured using RNAseq. Red and blue colors indicate higher and lower mean expression, respectively, as measured by row standardized Z-scores (n=6 biologically independent mice). (b) Volcano plot of the Pearson correlation coefficient p-value vs Pearson correlation coefficient. Positively-associated genes were labelled with orange and the negatively-associated genes were labelled with blue. The p=0.05 was marked with red dash line (n=6 biologically independent mice). (c) Partial list of the top enriched

pathways (KEGG) positively (red) and negatively (blue) correlated with BCAA intake. Data are from males and females combined, collected at 15 months of age (n=6 biologically independent mice). For (a,b) Pearson's correlation was used.

Europe PMC Funders Author Manuscripts

Europe PMC Funders Author Manuscripts

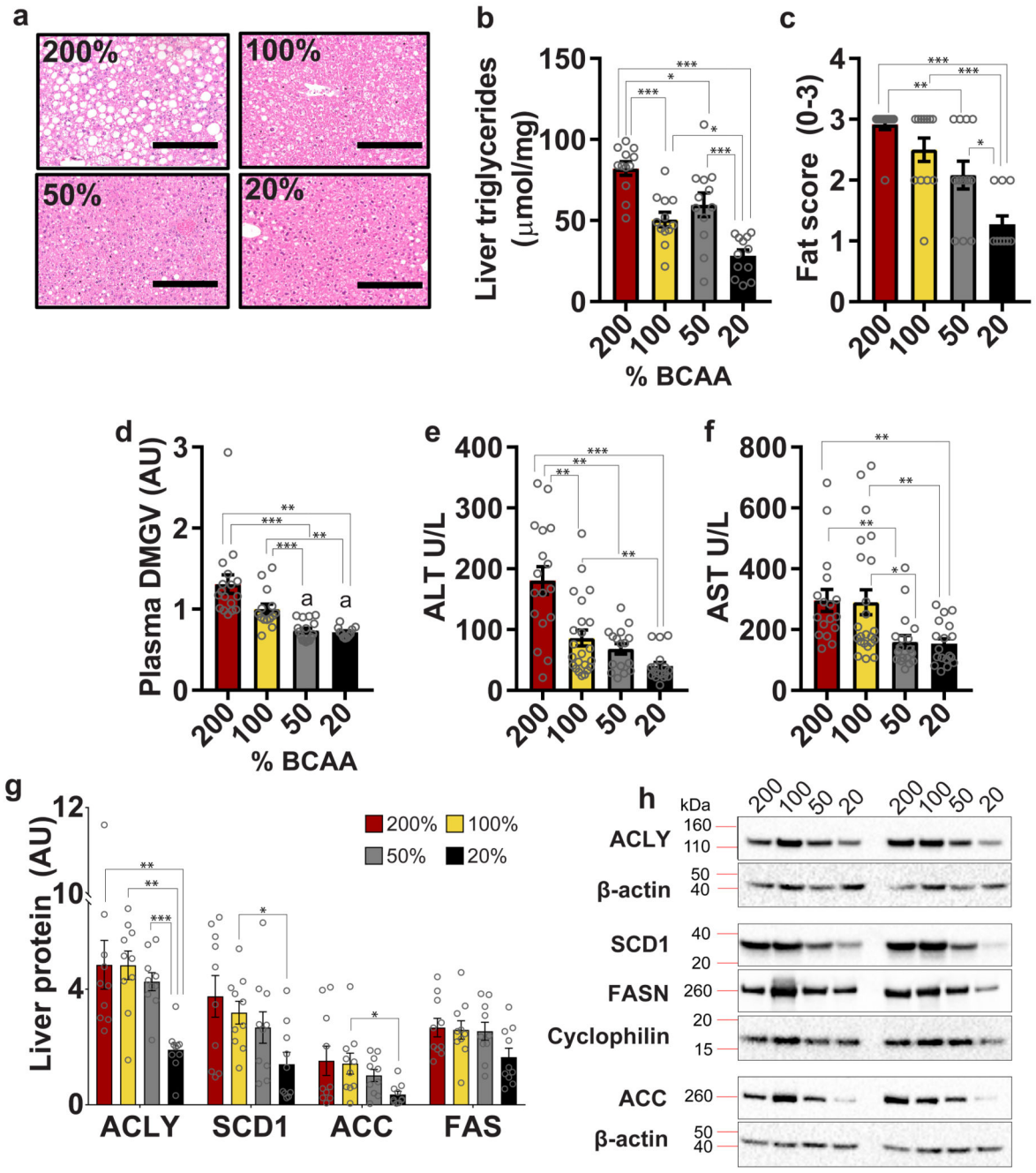

Fig. 5. Dietary BCAA imbalance promotes hepatosteatosis and *de novo* lipogenesis

(a) Representative H&E stains of livers (n=12 biologically independent mice, assessed once by four independent observers blinded to the dietary treatment groups). (b) Liver triglycerides (n=12 biologically independent mice for all groups), (c) Fat score (200%, 100% and 50%, n=12; 20%, n=11 biologically independent mice) and circulating levels of (d) DMGV, a novel metabolite marker for hepatosteatosis, are increased on high BCAA diets (200%, n=17; 100%, n=14; 50%, n=16; 20%, n=11 biologically independent mice). Liver function tests as indicated by plasma (e) ALT levels (200%, n=17; 100%, n=23; 50%, n=17;

20%, n=15 biologically independent mice) and (f) AST (200%, n=17; 100%, n=14; 50%, n=18; 20%, n=18 biologically independent mice). (g) Markers of *de novo* lipogenesis in liver quantified using western blot (n=10 biologically independent mice) with (h) representative images quantified once using 10 biologically independent mice. ACLY: ATP-citrate lyase; SCD1: stearoyl-coA desaturase-1; FAS: fatty acid synthase; ACC: acetyl-coA carboxylase. Data are from males and females combined, collected at 15 months of age. For all bar graphs, ANOVA for normal and log-normal data, and Kruskal Wallis tests for non-normal data, were used to determine significant differences between groups. Pairwise comparisons amongst diets for normal and log-normal data were made using t-tests (two-sided). For non-normal data, pairwise comparisons amongst diets were made using Kruskal Wallis test. All bars indicate means ± SEM. *p≤0.05, **p≤0.01, ***p≤0.001 based on posthoc analysis following correction for multiple testing.

Europe PMC Funders Author Manuscripts

Europe PMC Funders Author Manuscripts

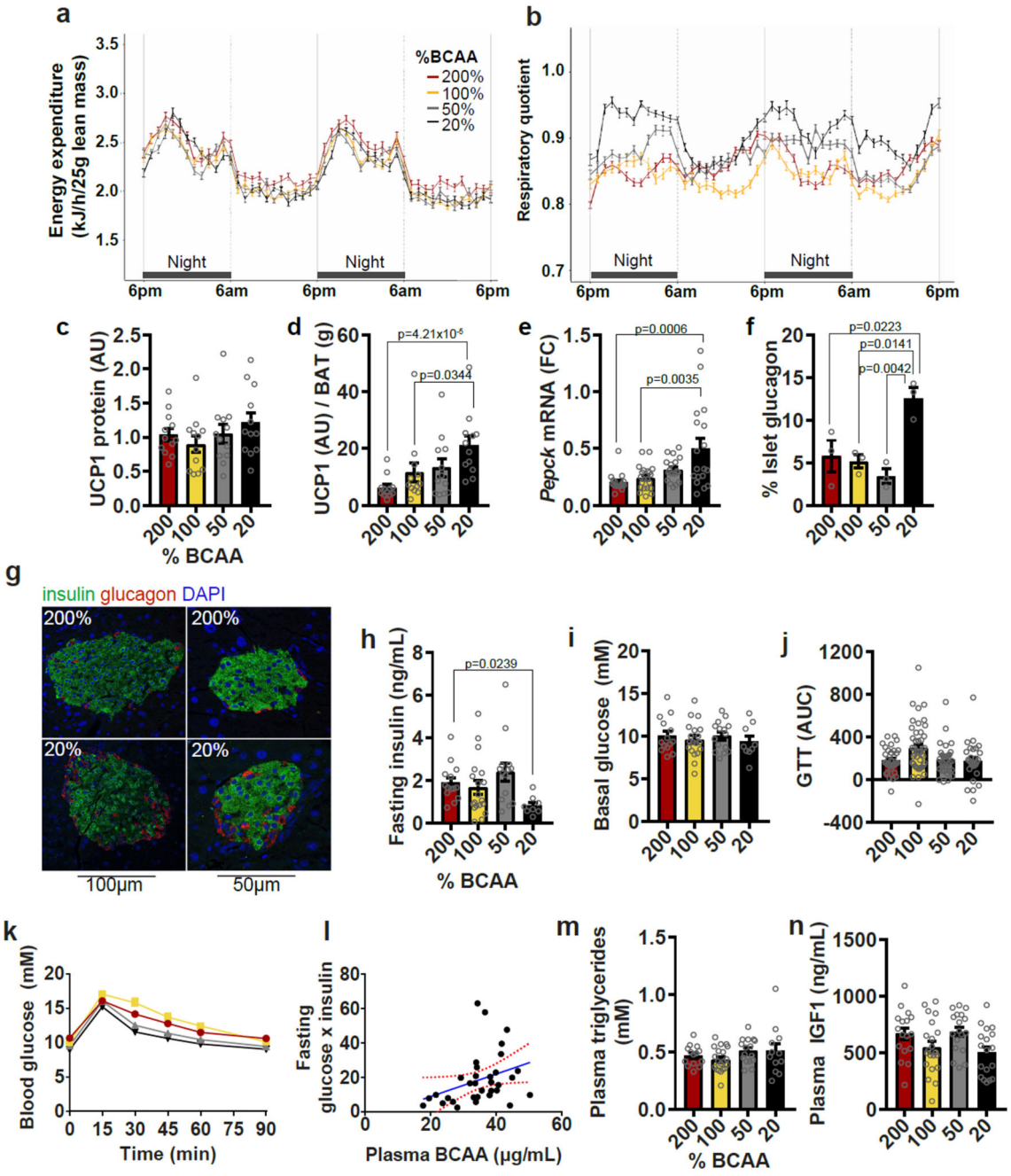

Fig. 6. Dietary amino acid imbalance alters whole body metabolism

(a) Energy expenditure and (b) Respiratory quotient (RQ) (200%, 50% and 20%, n=12; 100%, n=16 biologically independent mice). Energy expenditure and RQ were measured in individual animals over 2 day and 2 night cycles using metabolic cages. (c) UCP1 protein expression in BAT (n=12 biologically independent mice) and (d) UCP1 protein per g of BAT mass (n=12 biologically independent mice). All western blots were standardized to contain 25ug of protein. (e) *Pepck* mRNA expression in liver (200%, n=17; 100%, n=21; 50% and 20%, n=18 biologically independent mice). (f) Glucagon content in pancreatic islets (n=3

Europe PMC Funders Author Manuscripts

mice) and (g) representative images of BCAA200 and BCAA20 islets visualized by immunohistochemistry, conducted once with 3 independent mice). Glucose metabolism is shown by (h) fasting insulin levels (200%, n=14; 100%, n=19; 50%, n=14; 20%, n=8 mice), (i) basal glucose levels (200%, n=14;, 100%, n=19; 50%, n=15; 20%, n=9 mice) and (j,k) the area under the curve (AUC) from glucose tolerance tests (GTT) (200%, n=33; 100%, n=44; 50%, n=33%; 20%, n=27 mice). (l) The relationship between plasma BCAAs and the product of fasting glucose and insulin, an index of insulin sensitivity (p=0.054; r=0.115; Pearson's correlation; n=33 mice). Red lines show the 95% confidence interval. Plasma (m) triglycerides (200%, n=14, 100%, n=20; 50%, n=16; 20%, n=12 mice) and (n) IGF1 (200%, n=17; 100%, n=21, 50% and 20%, n=18 mice) were measured. For all bar graphs, ANOVA for normal and log-normal data, and Kruskal Wallis tests for non-normal data, were used to determine significant differences between groups. Pairwise comparisons amongst diets for normal and log-normal data were made using t-tests (two-sided). For non-normal data, pairwise comparisons amongst diets were made using Kruskal Wallis test. All bars indicate means ± SEM. *p≤0.05, **p≤0.01, ***p≤0.001 based on posthoc analysis following correction for multiple testing.

Europe PMC Funders Author Manuscripts

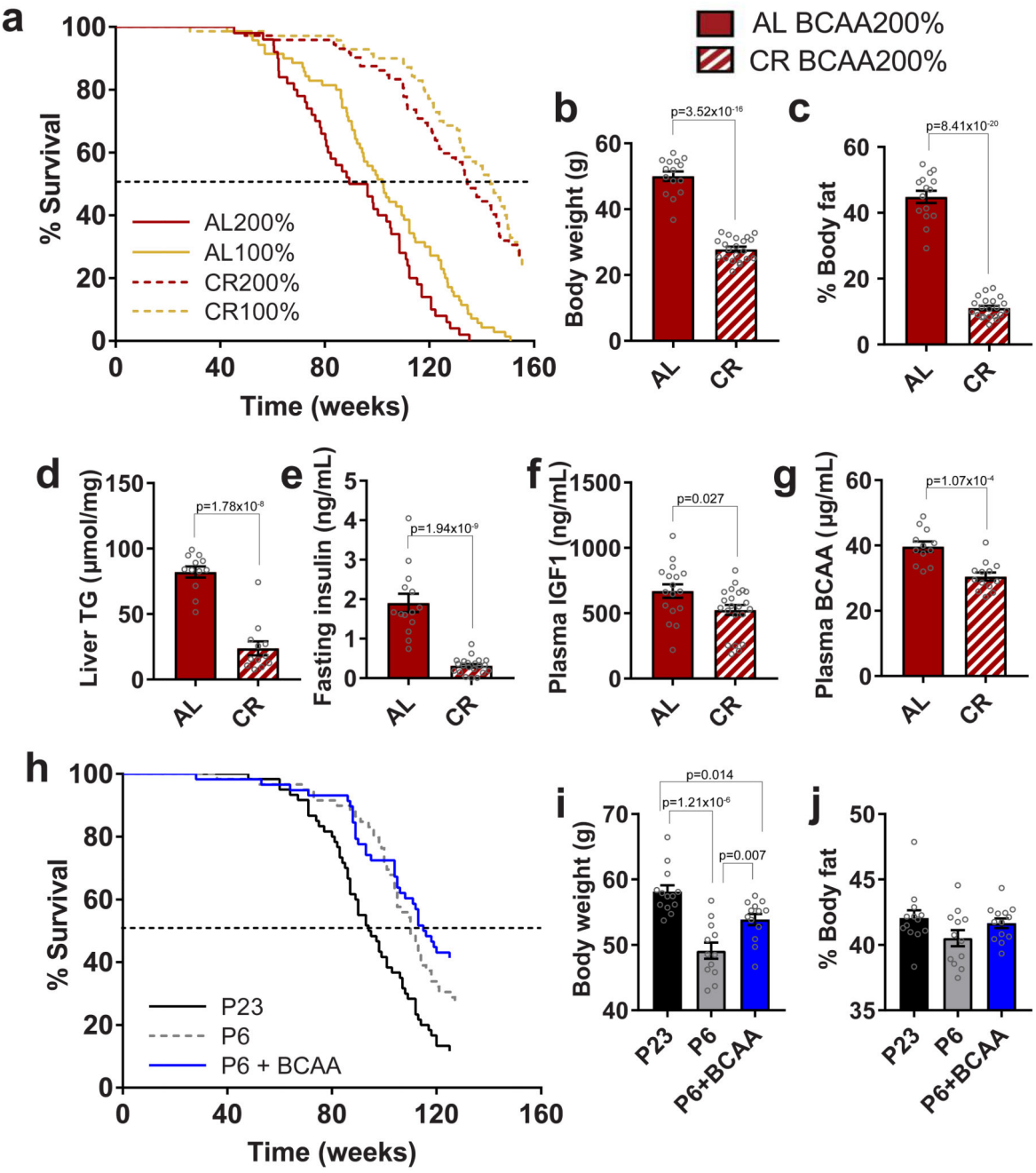

Fig. 7. Preventing hyperphagia on high BCAA diets averts metabolic and lifespan costs

(a) Survival curves of *ad libitum*-fed (AL) and 20% calorically restricted (CR) mice. Data from AL animals are replotted from Fig. 1n and shown here for direct lifespan comparison to CR. (b) Body weight (AL, n=15; CR, n=21 independent cages) and (c) % body fat (AL, n=15; CR, n=21 independent cages) of 15 month-old mice fed a BCAA200 diet at either AL or CR conditions. (d) Liver triglyceride content (TG) (n=12 biologically independent mice) and plasma analysis of (e) fasting insulin (AL, n=14; CR, n=21 independent cages), (f) IGF1 (AL, n=17; CR, n=22 independent cages) and (g) BCAA (AL, n=12; CR, n=13 biologically

independent mice). (h) Survival curves of mice pair fed with an exome-matched diet of either 23% protein, 6% protein, of 6%+BCAAs. (i) Body weights and (j) % body fat for animals at 12 months of age (P23, n=13; P6, n=12; P6+BCAA, n=13 biologically independent mice). For (b-g), two-sided t-tests were used. For (i,j), ANOVA and Tukey's multiple comparisons posthoc test were used. All bars indicate means ± SEM. *p≤0.05, **p≤0.01, ***p≤0.001 based on posthoc analysis following correction for multiple testing.

Europe PMC Funders Author Manuscripts